PLANE WAVE DISCONTINUOUS GALERKIN METHODS

C. J. GITTELSON*, R. HIPTMAIR†, AND I. PERUGIA‡

Abstract. We are concerned with a finite element approximation for time-harmonic wave propagation governed by the Helmholtz equation. The usually oscillatory behavior of solutions, along with numerical dispersion, render standard finite element methods grossly inefficient already in medium-frequency regimes. As an alternative, methods that incorporate information about the solution in the form of plane waves have been proposed. Among them the ultra weak variational formulation (UWVF) of Cessenat and Despres [O. CESSENAT AND B. DESPRES, *Application of an ultra weak variational formulation of elliptic PDEs to the two-dimensional Helmholtz equation*, SIAM J. Numer. Anal., 35 (1998), pp. 255–299.].

We identify the UWVF as representative of a class of Trefftz-type discontinuous Galerkin methods that employs trial and test spaces spanned by local plane waves. In this paper we give a priori convergence estimates for the h-version of these plane wave discontinuous Galerkin methods. To that end, we develop new inverse and approximation estimates for plane waves in two dimensions and use these in the context of duality techniques. Asymptotic optimality of the method in a mesh dependent norm can be established. However, the estimates require a minimal resolution of the mesh beyond what it takes to resolve the wavelength. We give numerical evidence that this requirement cannot be dispensed with. It reflects the presence of numerical dispersion.

Key words. Wave propagation, finite element methods, discontinuous Galerkin methods, plane waves, ultra weak variational formulation, duality estimates, numerical dispersion

AMS subject classifications. 65N15, 65N30, 35J05

1. Introduction. This paper is devoted to the numerical analysis of volumetric discretization schemes for the following model boundary value problem for the Helmholtz equation:

$$\begin{aligned}
-\Delta u - \omega^2 u &= f && \text{in } \Omega, \\
\nabla u \cdot \boldsymbol{n} + i\omega\, u &= g && \text{on } \partial\Omega.
\end{aligned} \tag{1.1}$$

Here, Ω is a bounded polygonal/polyhedral Lipschitz domain in $\mathbb{R}^d$, $d = 2, 3$, and $\omega > 0$ denotes a fixed wave number (the corresponding wavelength is $\lambda = 2\pi/\omega$). The right hand side f is a source term in $H^{-1}(\Omega)$, $\boldsymbol{n}$ is the outer normal unit vector to $\partial\Omega$, and i is the imaginary unit. Inhomogeneous first order absorbing boundary conditions in the form of impedance boundary conditions are used in (6.2), with boundary data $g \in H^{-1/2}(\partial\Omega)$.

Denoting by $(\cdot, \cdot)$ the standard complex $L^2(\Omega)$–inner product, namely, $(u, v) = \int_\Omega u\,\overline{v}\,\mathrm{d}V$, the variational formulation of (1.1) reads as follows[1]: find $u \in H^1(\Omega)$ such that, for all $v \in H^1(\Omega)$,

$$(\nabla u, \nabla v) - \omega^2 (u, v) + i\omega \int_{\partial\Omega} u\,\overline{v}\,\mathrm{d}S = (f, v) + \int_{\partial\Omega} g\,\overline{v}\,\mathrm{d}S. \tag{1.2}$$

*SAM, ETH Zurich, CH-8092 Zürich, giclaude@student.ethz.ch

‡Dipartimento di Matematica, Università di Pavia, ilaria.perugia@unipv.it

[1]For a bounded domain $D \subset \mathbb{R}^d$, $d = 1, 2, 3$, we denote by $H^s(D)$, $s \in \mathbb{N}_0$, the standard Sobolev space of order s of complex-valued functions, and by $\|\cdot\|_{s,D}$ the usual Sobolev norm. For $s = 0$, we write $L^2(D)$ in lieu of $H^0(D)$. We also use $\|\cdot\|_{s,D}$ to denote the norm for the space $(H^s(D))^d$.

Existence and uniqueness of solutions of (1.2) is well establish, see, e.g., [20, Section 8.1].

The Galerkin discretization of (1.2) by means of standard piecewise polynomial $H^1(\Omega)$–conforming finite elements is straightforward. Yet, it may deliver sufficient accuracy only at prohibitive costs. For two reasons: firstly, solutions of (6.2) tend to oscillate on the scale of the wavelength $\lambda = 2\pi/\omega$, which entails fine meshes or high polynomial degrees in the case of piecewise polynomial approximation. Secondly, low order finite element schemes are also haunted by the so-called *pollution effect*, that is, a widening gap between best approximation error and Galerkin discretization error for increasing wavenumbers, see [4, 18]. Spectral Galerkin methods can apparently avoid the pollution effect, at the expense of non-locality of the discretization, see [1]. The pollution effect is closely linked to the notion of *numerical dispersion*: we observe that plane waves $\boldsymbol{x} \mapsto \exp(i\omega\boldsymbol{d}\cdot\boldsymbol{x})$, $|\boldsymbol{d}| = 1$, are solutions of the homogeneous Helmholtz equation $-\Delta u - \omega^2 u = 0$; when the discretized operator is examined (in a periodic setting), its kernel functions turn out to be similar plane waves but with a different wavelength.

It is a natural idea to incorporate "knowledge" about both the oscillatory character of solutions and their intrinsic wavelength into a discretization of (6.2). This has been pursued in many ways, mainly by building trial spaces based on plane waves. This has been attempted in the partition of unity (PUM) finite element method [3, 14, 19, 20, 22], the discontinuous enrichment approach [12, 13, 26], and in the context of least squares approaches [21, 25].

Arguably, the most "exotic" among the plane wave methods is the ultra-weak variational formulation (UWVF) introduced by Cessenat and Despres [9–11]. It owes its name to the twofold integration by parts underlying its original formulation, which features impedance traces on cell boundaries as unknowns in the variational formulation. Cessenat and Despres managed to establish existence and uniqueness of solutions of the UWVF, but failed to give meaningful a priori error estimates. On the other hand, extensive numerical experiments mainly conducted by P. Monk and collaborators indicate reliable convergence [16, 17] for a wide range of wave propagation problems (without volume sources). This carries over to the extension of the method to Maxwell's equations [15].

Fresh analysis was made possible by the discovery that the UWVF can be recast as a special discontinuous Galerkin (DG) method for (6.2) with trial and test spaces supplied by local plane wave spaces. This relationship gradually emerged, *cf.* [15], and is made fully explicit in Section 3 of this article and in a paper by A. Buffa and P. Monk [7], which was written parallel to ours. The big gain from this new perspective is that powerful techniques of DG analysis can be harnessed for understanding the convergence properties of the UWVF. This was done in [7] building on estimates already established by Cessenat and Despres. In the present paper the relationship of UWVF and DG paves the way for adapting the convergence theory of elliptic DG methods [8] combined with duality techniques [5, 23]. We point out that this entailed a slight modification of the UWVF in order to enhance its stability.

Thus, we obtain a priori h–asymptotic estimates in both a mesh-dependent broken H^1–norm and the L^2–norm, see Section 5. The estimates target the case of uniform mesh refinement keeping the resolution of local trial spaces fixed, the so-called h–version of volumetric discretization schemes. h–asymptotic quasi-optimality with ω–uniform constants is established, but under daunting circumstances: writing h for the global meshwidth, we have to assume that $h\omega^2$ is sufficiently small, which amounts

to the pollution effect rearing its head again. Basically we end up with the same requirement of over-resolving the wavelength as stipulated by the usual error estimates for piecewise linear globally continuous finite elements.

In short, theory dismisses the UWVF as miracle cure for numerical dispersion and simple numerical experiments carry the same message, see Section 7. Nevertheless plane wave DG method for (6.2) can be viable when used wisely. It is not advisable to try and improve accuracy by refining the mesh. Rather, the cell size should be linked to the wavelength and the number of plane wave directions should be increased. In fact, it is large cells and large local spaces that are preferred in practical applications of the method.

Hence, the asymptotics considered in the present paper and in [7, 9] may not be the right one. Nevertheless, we believe that investigation of h–version convergence is an essential first step in understanding the more interesting p–version of plane wave Galerkin methods. Moreover, already the case of h–refinement forced us to develop some theoretical tools which are certainly of interest in their own right: *(i)* construction of a basis for plane wave spaces that remains stable for small wavenumbers (see Section 4.1); *(ii)* inverse estimates and projection error estimates for plane waves (see Section 4.2); *(iii)* new variants of duality arguments (see Section 5).

The outline of the paper is as follows: after recalling the UWVF in Section 2, we rewrite it in Section 3 as a (primal) mixed DG method; Section 4 contains the definition of a stable basis for plane wave spaces and some related key results (inverse and projection error estimates) used in the convergence analysis developed in Section 5. Section 6 deals with the duality estimate in the one-dimensional case. Finally, numerical results demonstrating the predicted h-convergence sharpness are presented in Section 7.

2. Ultra weak variational formulation. The main ingredients of the ultra weak variational formulation-based method introduced by Cessenat and Despres in [9] are the following: *(i)* a partition $\mathcal{T}_h$ of Ω into subdomains K of diameters h_K; *(ii)* subdomainwise ultra weak variational formulation of (1.1) (integrate by parts twice the second order term in the first equation of (1.1) on each K); *(iii)* finite dimensional trial and test spaces spaces V_h made of p plane waves on each $K \in \mathcal{T}_h$.

Therefore, let $\mathcal{T}_h$ be a partition of Ω into polyhedral subdomains K of diameters h_K with possible hanging nodes. Let $\mathcal{F}_h$ be the skeleton of the partition $\mathcal{T}_h$, and define $\mathcal{F}_h^{\mathcal{B}} = \mathcal{F}_h \cap \partial\Omega$ and $\mathcal{F}_h^{\mathcal{I}} = \mathcal{F}_h \setminus \mathcal{F}_h^{\mathcal{B}}$. Finally, we will denote by ∇_h and Δ_h the elementwise application of the operators ∇ and Δ, respectively.

The method of Cessenat and Despres as published in [9] is usually stated in terms of unknown functions on $\mathcal{F}_h$, see also [7, Formula 19]. Yet it can be equivalently stated as follows: find $u_h \in V_h$ such that, for all $v_h \in V_h$,

$$
\begin{aligned}
\sum_{K \in \mathcal{T}_h} &\int_{\partial K} (-\nabla u_h \cdot \boldsymbol{n} + i\omega u_h)(\overline{-\nabla v_h \cdot \boldsymbol{n} + i\omega v_h}) \, \mathrm{d}S \\
&- \int_{\mathcal{F}_h^{\mathcal{I}}} (-\nabla u_h^- \cdot \boldsymbol{n}^- + i\omega u_h^-)(\overline{\nabla v_h^+ \cdot \boldsymbol{n}^+ + i\omega v_h^+}) \, \mathrm{d}S \\
&- \int_{\mathcal{F}_h^{\mathcal{I}}} (-\nabla u_h^+ \cdot \boldsymbol{n}^+ + i\omega u_h^+)(\overline{\nabla v_h^- \cdot \boldsymbol{n}^- + i\omega v_h^-}) \, \mathrm{d}S \\
&= -2i\omega\,(f, v_h) + \int_{\mathcal{F}_h^{\mathcal{B}}} g(\overline{\nabla v_h \cdot \boldsymbol{n} + i\omega v_h}) \, \mathrm{d}S \,,
\end{aligned}
\tag{2.1}
$$

where the superscripts $^+$ and $^-$ refer to quantities from the two different elements sharing the considered interior face (see [9, Formula (1.4)] and [17, Formula 10]).

Following [15], it is possible to show that the method by Cessenat and Despres can be recovered by writing the second order problem as a first order system, and then discretizing this system by using a discontinuous Galerkin (DG) method with flux splitting approach (classical upwind DG method). Here, we follow a slightly different approach and see that the method by Cessenat and Despres is a particular method of the general class of DG methods presented in [8]. A similar perspective is adopted in [7, Sect. 2].

3. Mixed discontinuous Galerkin approach. In order to derive the method by Cessenat and Despres as a particular representative of the general class of DG methods presented in [8], we introduce the auxiliary variable $\boldsymbol{\sigma} := \nabla u / i\omega$ and write problem (1.1) as a first order system:

$$
\begin{aligned}
i\omega\,\boldsymbol{\sigma} &= \nabla u & &\text{in } \Omega, \\
i\omega\,u - \nabla\cdot\boldsymbol{\sigma} &= \frac{1}{i\omega}\,f & &\text{in } \Omega, \\
i\omega\boldsymbol{\sigma}\cdot\boldsymbol{n} + i\omega\,u &= g & &\text{on } \partial\Omega.
\end{aligned}
\tag{3.1}
$$

Now, introduce a partition $\mathcal{T}_h$ of Ω into subdomains K, and proceed as in [8]. By multiplying the first and second equations of (3.1) by smooth test functions $\boldsymbol{\tau}$ and v, respectively, and integrating by parts on each K, we obtain

$$
\begin{aligned}
\int_K i\omega\,\boldsymbol{\sigma}\cdot\overline{\boldsymbol{\tau}}\,\mathrm{d}V + \int_K u\,\overline{\nabla\cdot\boldsymbol{\tau}}\,\mathrm{d}V - \int_{\partial K} u\,\overline{\boldsymbol{\tau}\cdot\boldsymbol{n}}\,\mathrm{d}S &= 0 \quad \forall\boldsymbol{\tau}\in\mathbf{H}(\mathrm{div};K) \\
\int_K i\omega\,u\,\overline{v}\,\mathrm{d}V + \int_K \boldsymbol{\sigma}\cdot\overline{\nabla v}\,\mathrm{d}V - \int_{\partial K} \boldsymbol{\sigma}\cdot\boldsymbol{n}\,\overline{v}\,\mathrm{d}S &= \frac{1}{i\omega}\int_K f\,\overline{v}\,\mathrm{d}V \quad \forall v\in H^1(K)\,.
\end{aligned}
\tag{3.2}
$$

Introduce discontinuous *discrete* function spaces $\boldsymbol{\Sigma}_h$ and V_h; replace $\boldsymbol{\sigma},\boldsymbol{\tau}$ by $\boldsymbol{\sigma}_h,\boldsymbol{\tau}_h\in\boldsymbol{\Sigma}_h$ and u,v by $u_h,v_h\in V_h$. Then, approximate the traces of u and $\boldsymbol{\sigma}$ across interelement boundaries by the so-called *numerical fluxes* denoted by $\widehat{u}_h$ and $\widehat{\boldsymbol{\sigma}}_h$, respectively (see, e.g., [2] for details) and obtain

$$
\begin{aligned}
\int_K i\omega\,\boldsymbol{\sigma}_h\cdot\overline{\boldsymbol{\tau}}_h\,\mathrm{d}V + \int_K u_h\,\overline{\nabla\cdot\boldsymbol{\tau}}_h\,\mathrm{d}V - \int_{\partial K} \widehat{u}_h\,\overline{\boldsymbol{\tau}_h\cdot\boldsymbol{n}}\,\mathrm{d}S &= 0 \quad \forall\boldsymbol{\tau}_h\in\boldsymbol{\Sigma}_h(K) \\
\int_K i\omega\,u_h\,\overline{v}_h\,\mathrm{d}V + \int_K \boldsymbol{\sigma}_h\cdot\overline{\nabla v}_h\,\mathrm{d}V - \int_{\partial K} \widehat{\boldsymbol{\sigma}}_h\cdot\boldsymbol{n}\,\overline{v}_h\,\mathrm{d}S &= \frac{1}{i\omega}\int_K f\,\overline{v}_h\,\mathrm{d}V \quad \forall v_h\in V_h(K)\,.
\end{aligned}
\tag{3.3}
$$

At this point, in order to complete the the definition of classical DG methods, one "simply" needs to choose the numerical fluxes $\widehat{u}_h$ and $\widehat{\boldsymbol{\sigma}}_h$ (notice that only the normal component of $\widehat{\boldsymbol{\sigma}}_h$ is needed).

Here, in order to recover the method by Cessenat and Despres, we integrate back by parts the first equation of (3.3):

$$
\int_K \boldsymbol{\sigma}_h\cdot\overline{\boldsymbol{\tau}}_h\,\mathrm{d}V = \frac{1}{i\omega}\int_K \nabla u_h\cdot\overline{\boldsymbol{\tau}}_h\,\mathrm{d}V - \frac{1}{i\omega}\int_{\partial K} (u_h - \widehat{u}_h)\,\overline{\boldsymbol{\tau}_h\cdot\boldsymbol{n}}\,\mathrm{d}S\,.
\tag{3.4}
$$

Assume $\nabla_h V_h \subseteq \boldsymbol{\Sigma}_h$ and take $\boldsymbol{\tau}_h = \nabla v_h$ in each element. Insert the resulting expression for $\int_K \boldsymbol{\sigma}_h \cdot \overline{\nabla v_h} \, dV$ into the second equation of (3.3). We get

$$\int_K (\nabla u_h \cdot \nabla \overline{v}_h - \omega^2 u_h \overline{v}_h) \, dV - \int_{\partial K} (u_h - \widehat{u}_h) \, \overline{\nabla v_h \cdot \boldsymbol{n}} \, dS - \int_{\partial K} i\omega \widehat{\boldsymbol{\sigma}}_h \cdot \boldsymbol{n} \, \overline{v}_h \, dS = \int_K f \, \overline{v}_h \, dV \ .$$
(3.5)

Notice that the formulation (3.5) is equivalent to (3.3) in the sense that their u_h solution components coincide and the $\boldsymbol{\sigma}_h$ solution component of (3.3) can be recovered from u_h by using (3.4).

Another equivalent formulation can be obtained by integrating by parts once more the first term in (3.5) (notice that the boundary term appearing in this integration by parts cancels out with a boundary term already present in (3.5)):

$$\int_K (\overline{-\Delta v_h - \omega^2 v_h}) \, u_h \, dV + \int_{\partial K} \widehat{u}_h \, \overline{\nabla v_h \cdot \boldsymbol{n}} \, dS - \int_{\partial K} i\omega \widehat{\boldsymbol{\sigma}}_h \cdot \boldsymbol{n} \, \overline{v}_h \, dS = \int_K f \, \overline{v}_h \, dV \ . \quad (3.6)$$

By taking Trefftz-type test functions v_h in (3.6) such that, for all $K \in \mathcal{T}_h$,

$$-\Delta v_h - \omega^2 v_h = 0 \qquad \text{in } K \ ,$$

formulation (3.6) simply becomes

$$\int_{\partial K} \widehat{u}_h \, \overline{\nabla v_h \cdot \boldsymbol{n}} \, dS - \int_{\partial K} i\omega \widehat{\boldsymbol{\sigma}}_h \cdot \boldsymbol{n} \, \overline{v}_h \, dS = \int_K f \, \overline{v}_h \, dV \ . \qquad (3.7)$$

By properly choosing the numerical fluxes in (3.7), we can recover the original method by Cessenat and Despres (2.1). To give the details, it is convenient to adopt the notation used in the description of discontinuous Galerkin methods: let u_h and $\boldsymbol{\sigma}_h$ be a piecewise smooth function and vector field on $\mathcal{T}_h$, respectively. On $\partial K^- \cap \partial K^+$, we define

the averages: $\{\!\{u_h\}\!\} := \frac{1}{2}(u_h^+ + u_h^-)$, $\{\!\{\boldsymbol{\sigma}_h\}\!\} := \frac{1}{2}(\boldsymbol{\sigma}_h^+ + \boldsymbol{\sigma}_h^-)$,

the jumps: $[\![u_h]\!]_N := u_h^+ \boldsymbol{n}^+ + u_h^- \boldsymbol{n}^-$, $[\![\boldsymbol{\sigma}_h]\!]_N := \boldsymbol{\sigma}_h^+ \cdot \boldsymbol{n}^+ + \boldsymbol{\sigma}_h^- \cdot \boldsymbol{n}^-$.

Then, the method by Cessenat and Despres is obtained by choosing the numerical fluxes in (3.7) as follows: on $\partial K^- \cap \partial K^+ \subset \mathcal{F}_h^{\mathcal{I}}$, we define

$$\widehat{\boldsymbol{\sigma}}_h = \frac{1}{i\omega} \{\!\{\nabla_h u_h\}\!\} - \frac{1}{2} \, [\![u_h]\!]_N \ ,$$
$$\widehat{u}_h = \{\!\{u_h\}\!\} - \frac{1}{2i\omega} \, [\![\nabla_h u_h]\!]_N \ ,$$
(3.8)

and on $\partial K \cap \partial \Omega \subset \mathcal{F}_h^{\mathcal{B}}$, we define

$$\widehat{\boldsymbol{\sigma}}_h = \frac{1}{i\omega} \nabla_h u_h - \frac{1}{2} \left(\frac{1}{i\omega} \nabla_h u_h + u_h \boldsymbol{n} - \frac{1}{i\omega} g \boldsymbol{n} \right) ,$$
$$\widehat{u}_h = u_h - \frac{1}{2} \left(\frac{1}{i\omega} \nabla_h u_h \cdot \boldsymbol{n} + u_h - \frac{1}{i\omega} g \right) \ .$$
(3.9)

In fact, multiply equation (3.7) by $2i\omega$ and sum over all elements:

$$\sum_{K \in \mathcal{T}_h} \int_{\partial K} \left(2i\omega \widehat{u}_h \, \overline{\nabla v_h \cdot \boldsymbol{n}} + 2i\omega \widehat{\boldsymbol{\sigma}}_h \cdot \boldsymbol{n} \, \overline{i\omega v_h} \right) dS = 2i\omega(f, v_h) \ .$$

Now, plug in the fluxes defined in (3.8)–(3.9) and, by denoting with the superscript $^{\text{ext}}$ the quantities taken from the neighbors of the considered element K (obviously, $\boldsymbol{n}^{\text{ext}} = -\boldsymbol{n}$), we can write

$$
\sum_K \Big[\int_{\partial K \setminus \partial \Omega} \big[(i\omega u_h + i\omega u_h^{\text{ext}} - \nabla u_h \cdot \boldsymbol{n} - \nabla u_h^{\text{ext}} \cdot \boldsymbol{n}^{\text{ext}}) \overline{\nabla v_h \cdot \boldsymbol{n}}
$$
$$
+ (\nabla u_h \cdot \boldsymbol{n} - \nabla u_h^{\text{ext}} \cdot \boldsymbol{n}^{\text{ext}} - i\omega u_h + i\omega u_h^{\text{ext}}) \overline{i\omega v_h} \big] \, \mathrm{d}S
$$
$$
+ \int_{\partial K \cap \partial \Omega} \big[(i\omega u_h - \nabla u_h \cdot \boldsymbol{n} + g) \overline{\nabla v_h \cdot \boldsymbol{n}}
$$
$$
+ (\nabla u_h \cdot \boldsymbol{n} - i\omega u_h + g) \overline{i\omega v_h} \big] \, \mathrm{d}S \Big] = 2i\omega (f, v_h) \,,
$$

from which, by rearranging the terms, we obtain (2.1).

We modify the fluxes in (3.8)–(3.9) by multiplying $[\![u_h]\!]_N$ and $[\![\nabla_h u_h]\!]_N$ in (3.8) by mesh dependent coefficients. In order to do that, we define the local mesh size function h on $\mathcal{F}_h^{\mathcal{I}}$ by $\mathsf{h}(\boldsymbol{x}) = \min\{h_{K^-}, h_{K^+}\}$ if $\boldsymbol{x}$ is in the interior of $\partial K^- \cap \partial K^+$. Mimicking the general form of numerical fluxes introduced in [8], the primal formulation we will analyze is obtained by choosing the numerical fluxes in (3.7) as follows: on $\partial K^- \cap \partial K^+ \subset \mathcal{F}_h^{\mathcal{I}}$, we define

$$
\widehat{\boldsymbol{\sigma}}_h = \frac{1}{i\omega} \{\!\{\nabla_h u_h\}\!\} - \alpha \, [\![u_h]\!]_N - \frac{\boldsymbol{\gamma}}{i\omega} \, [\![\nabla_h u_h]\!]_N,
$$
$$
\widehat{u}_h = \{\!\{u_h\}\!\} + \boldsymbol{\gamma} \cdot [\![u_h]\!]_N - \frac{\beta}{i\omega} \, [\![\nabla_h u_h]\!]_N,
\tag{3.10}
$$

and on $\partial K \cap \partial \Omega \subset \mathcal{F}_h^{\mathcal{B}}$, we define

$$
\widehat{\boldsymbol{\sigma}}_h = \frac{1}{i\omega} \nabla_h u_h - (1 - \delta) \left(\frac{1}{i\omega} \nabla_h u_h + u_h \, \boldsymbol{n} - \frac{1}{i\omega} g \, \boldsymbol{n} \right),
$$
$$
\widehat{u}_h = u_h - \delta \left(\frac{1}{i\omega} \nabla_h u_h \cdot \boldsymbol{n} + u_h - \frac{1}{i\omega} g \right),
\tag{3.11}
$$

with parameters $\alpha > 0$, $\beta \geq 0$, $\boldsymbol{\gamma}$ and $0 < \delta < 1$ to be chosen.

The original method by Cessenat and Després [9] is recovered by choosing

$$
\alpha = 1/2 \,, \qquad \beta = 1/2 \,, \qquad \boldsymbol{\gamma} = \boldsymbol{0} \,, \qquad \delta = 1/2 \,.
$$

Yet, this choice lacks essential stability properties needed for the analysis of Sect. 5. Thus, we focus on a restricted class of primal methods where the parameters in the definition of the numerical fluxes (3.10) and (3.11) are as follows:

$$
\alpha = \mathsf{a}/\omega\mathsf{h} \,, \qquad \beta = \mathsf{b}\omega\mathsf{h} \,, \qquad \boldsymbol{\gamma} = \boldsymbol{0} \,, \qquad \delta = \mathsf{d}\omega\mathsf{h} \,,
\tag{3.12}
$$

with $\mathsf{a} \geq \mathsf{a}_{\min} > 0$ on $\mathcal{F}_h^{\mathcal{I}}$, $\mathsf{b} \geq 0$ on $\mathcal{F}_h^{\mathcal{I}}$ and $\mathsf{d} \geq 0$ on $\mathcal{F}_h^{\mathcal{B}}$, all independent of the mesh size and ω. Further assumptions on $\mathsf{a}_{\min}$ and d will be stated in Sect. 5.

REMARK 3.1. *One may also consider the Helmholtz boundary value problem with Dirichlet boundary conditions. In this case, for the boundary condition $u = g_D$ on $\partial\Omega$, the appropriate numerical fluxes for cell faces on $\partial\Omega$ are*

$$
\widehat{\boldsymbol{\sigma}}_h = \frac{1}{i\omega} \nabla_h u_h - \lambda \left(u_h \, \boldsymbol{n} - g_D \, \boldsymbol{n} \right),
$$
$$
\widehat{u}_h = g_D,
\tag{3.13}
$$

with a parameter $\lambda > 0$. In this case the boundary value problem lacks a unique solution for ω from an infinte discrete set resonant wave numbers. Thus, we skip pure Dirichlet boundary conditions, as well as pure Neumann boundary conditions, in the convergence analysis.

4. Plane waves. We restrict ourselves to the case $d = 2$ and to triangular meshes. Let $PW_\omega(\mathbb{R}^2)$ be the space of linear combinations of $p \in \mathbb{N}$ plane waves of wavelength $\frac{2\pi}{\omega}$, $\omega > 0$, in $\mathbb{R}^2$, i.e.,

$$PW_\omega(\mathbb{R}^2) = \{v \in C^\infty(\mathbb{R}^2) \,:\, v(\boldsymbol{x}) = \sum_{j=1}^{p} \alpha_j \exp(i\omega \boldsymbol{d}_j \cdot \boldsymbol{x}), \ \alpha_j \in \mathbb{C}\}\,, \qquad (4.1)$$

where the directions $\boldsymbol{d}_j \in \mathbb{R}^2$ are fixed, have unit length and are assumed to be different from each other. For simplicity, we suppress the dependence on $\{\boldsymbol{d}_j\}_{j=1}^{p}$ in the notation for $PW_\omega(\mathbb{R}^2)$. It goes without saying that every $v \in PW_\omega(\mathbb{R}^2)$ is a solution of the homogeneous Helmholtz equation $-\Delta v - \omega^2 v = 0$ in $\mathbb{R}^2$.

LEMMA 4.1. *With the abbreviation $e_k := \exp(i\omega \boldsymbol{d}_k \cdot)$ the set $\{e_k\}_{k=1}^{p}$ is a basis of $PW_\omega(\mathbb{R}^2)$ for all $\omega > 0$.*

Proof. Setting $\boldsymbol{x} = \boldsymbol{d}_k \xi$, $\xi \in \mathbb{R}$, we conclude from

$$\sum_{j=1}^{p} \alpha_j \exp(i\omega \boldsymbol{d}_j \cdot \boldsymbol{x}) = 0 \quad \forall \boldsymbol{x} \in \mathbb{R}^2\,, \qquad (4.2)$$

that

$$\alpha_k + \sum_{\substack{j=1 \\ j \neq k}}^{p} \alpha_j \exp(i\omega(\boldsymbol{d}_j \cdot \boldsymbol{d}_k - 1)\xi) = 0 \quad \forall \xi \in \mathbb{R}\,. \qquad (4.3)$$

As $\boldsymbol{d}_j \cdot \boldsymbol{d}_k < 1$ for $j \neq k$, this can only hold if $\alpha_k = 0$. $\square$

The drawback of this natural basis is that its vectors become "ever more linearly dependent" as $\omega \to 0$: obviously $e_k \to 1$ if $\omega \to 0$ uniformly on any compact set. For both numerical and theoretical purposes a basis that remains stable for $\omega \to 0$ is urgently needed. The construction of such a basis is carried out in Section 4.1 and inverse and projections estimates for plane wave functions are studied in Section 4.2.

4.1. Stable bases for plane waves. For reasons that will become apparent below, we restrict ourselves to odd $p = 2m + 1$, $m \in \mathbb{N}$; see Remark 4.3 below. For the direction vectors we may write $\boldsymbol{d}_k := \binom{\cos(\varphi_k)}{\sin(\varphi_k)}$, $\varphi_k \in [0, 2\pi[$, with $\varphi_k \neq \varphi_j$ for $k \neq j$. It is convenient to introduce the symbol

$$\mu_{l,k} := \begin{cases} 1 & \text{for } l = 1\,, \\ \cos(\frac{l}{2}\varphi_k) & \text{for even } l\,, \\ \sin(\frac{l-1}{2}\varphi_k) & \text{for odd } l \geq 3\,, \end{cases} \qquad l, k \in \mathbb{N}\,. \qquad (4.4)$$

Let $\boldsymbol{M}_p$ stand for the real $p \times p$–matrix $(\mu_{l,k})_{l,k=1}^p$. For $p = 2m+1$ it reads

$$\boldsymbol{M}_p := \begin{pmatrix} 1 & 1 & 1 & \cdots & \cdots & 1 \\ \cos(\varphi_1) & \cos(\varphi_2) & \cos(\varphi_3) & \cdots & \cdots & \cos(\varphi_p) \\ \sin(\varphi_1) & \sin(\varphi_2) & \sin(\varphi_3) & \cdots & \cdots & \sin(\varphi_p) \\ \cos(2\varphi_1) & \cos(2\varphi_2) & \cos(2\varphi_3) & \cdots & \cdots & \cos(2\varphi_p) \\ \sin(2\varphi_1) & \sin(2\varphi_2) & \sin(2\varphi_3) & \cdots & \cdots & \sin(2\varphi_p) \\ \vdots & \vdots & \vdots & & & \vdots \\ \cos(m\varphi_1) & \cos(m\varphi_2) & \cos(m\varphi_3) & \cdots & \cdots & \cos(m\varphi_p) \\ \sin(m\varphi_1) & \sin(m\varphi_2) & \sin(m\varphi_3) & \cdots & \cdots & \sin(m\varphi_p) \end{pmatrix} . \qquad (4.5)$$

LEMMA 4.2. *For odd p the matrix $\boldsymbol{M}_p \in \mathbb{R}^{p,p}$ from (4.5) is regular.*
Proof. If $\boldsymbol{M}_p^T \vec{\zeta} = 0$ for some $\vec{\zeta} \in \mathbb{R}^p$, then

$$\zeta_0 + \sum_{l=1}^m \left[\zeta_{2l-1} \cos(l\varphi_k) + \zeta_{2l} \sin(l\varphi_k) \right] = 0 \quad \text{for } k = 1, \ldots, p .$$

Hence, $\vec{\zeta}$ is the coefficient vector for a real valued trigonometric polynomial of degree m with $2m+1$ different zeros φ_k, $k = 1, \ldots, p$. This polynomial must be zero everywhere. □

The inverse of the matrix $\boldsymbol{M}_p$ will effect a transformation to a basis that remains *stable in the limit $\omega \to 0$.* We set $\alpha_k^{(j)} := \left(\boldsymbol{M}_p^{-1} \right)_{k,j}$, $1 \le k, j \le p$, and define

$$b_j := (i\omega)^{-\left[\frac{j}{2}\right]} \sum_{k=1}^p \alpha_k^{(j)} e_k . \qquad (4.6)$$

Since $\boldsymbol{M}_p$ is regular, $\{b_j\}_{j=1}^p$ will be a basis of $PW_\omega(\mathbb{R}^2)$, too.

The actual computation of b_j starts from the series expansion of the exponentials

$$\sum_{k=1}^p \alpha_k^{(j)} e_k(\boldsymbol{x}) = \sum_{n=0}^\infty \frac{1}{n!} (i\omega)^n \sum_{k=1}^p \alpha_k^{(j)} (\boldsymbol{d}_k \cdot \boldsymbol{x})^n , \qquad (4.7)$$

where summations may be interchanged due to the uniform convergence of the series. Next, we write $\boldsymbol{x} = \binom{x}{y}$ and use that

$$\left(\binom{\cos\varphi}{\sin\varphi} \cdot \boldsymbol{x} \right)^n = \sum_{j=0}^n \binom{n}{j} \cos^{n-j}(\varphi) \sin^j(\varphi) \, x^{n-j} y^j \qquad (4.8)$$

is a real trigonometric polynomial of degree n. Thus it can be expressed as a Fourier sum

$$\left(\binom{\cos\varphi}{\sin\varphi} \cdot \boldsymbol{x} \right)^n = \frac{\gamma_0^n(\boldsymbol{x})}{2} + \sum_{j=1}^n \left[\gamma_j^n(\boldsymbol{x}) \cos(j\varphi) + \sigma_j^n(\boldsymbol{x}) \sin(j\varphi) \right] , \qquad (4.9)$$

where

$$\gamma_j^n(\boldsymbol{x}) = \frac{1}{\pi} \int_{-\pi}^\pi \left(\binom{\cos\varphi}{\sin\varphi} \cdot \boldsymbol{x} \right)^n \cos(j\varphi) \, \mathrm{d}\varphi , \quad j = 0, \ldots, n , \qquad (4.10)$$

$$\sigma_j^n(\boldsymbol{x}) = \frac{1}{\pi} \int_{-\pi}^\pi \left(\binom{\cos\varphi}{\sin\varphi} \cdot \boldsymbol{x} \right)^n \sin(j\varphi) \, \mathrm{d}\varphi , \quad j = 1, \ldots, n . \qquad (4.11)$$

From (4.9) is it immediate that both $\gamma_j^n(\boldsymbol{x})$ and $\sigma_j^n(\boldsymbol{x})$ are homogeneous polynomials in x, y. We also find that

$$j + n \text{ odd} \quad \Rightarrow \quad \gamma_j^n(\boldsymbol{x}) = 0 \, , \quad \sigma_j^n(\boldsymbol{x}) = 0 \, . \tag{4.12}$$

In fact, by setting $z = x + iy$, we can write

$$\left(\begin{pmatrix} \cos \varphi \\ \sin \varphi \end{pmatrix} \cdot \boldsymbol{x} \right)^n = 2^{-n} \sum_{k=0}^{n} \binom{n}{k} \overline{z}^{n-k} z^k \exp(i(n-2k)\varphi).$$

Therefore, for even n, $\left(\begin{pmatrix} \cos \varphi \\ \sin \varphi \end{pmatrix} \cdot \boldsymbol{x} \right)^n$ has vanishing Fourier coefficients for odd indices, whereas, for odd n, it has vanishing Fourier coefficients for even indices. Formula (4.12) follows from the the fact that σ_j^n and γ_j^n are such trigonometric Fourier coefficients; see (4.9).

Moreover, for any $n \in \mathbb{N}$, the nonzero $\gamma_j^n(\boldsymbol{x})$, $\sigma_j^n(\boldsymbol{x})$ provide a basis of the space of two-variate homogeneous polynomials of degree n.

For the sake of simplicity, we set $\kappa_1^n(\boldsymbol{x}) := \gamma_0^n(\boldsymbol{x})/2$, $\kappa_{2j}^n(\boldsymbol{x}) := \gamma_j^n(\boldsymbol{x})$, $j = 1, \ldots, n$, for even j, and $\kappa_{2j+1}^n(\boldsymbol{x}) := \sigma_j^n(\boldsymbol{x})$ for odd j. Using (4.4) this permits us to rewrite

$$\left(\begin{pmatrix} \cos \varphi_k \\ \sin \varphi_k \end{pmatrix} \cdot \boldsymbol{x} \right)^n = \sum_{l=1}^{2n+1} \kappa_l^n(\boldsymbol{x})\mu_{l,k} \, . \tag{4.13}$$

We plug this into (4.7)

$$\sum_{k=1}^{p} \alpha_k^{(j)} e_k(\boldsymbol{x}) = \sum_{n=0}^{\infty} \frac{1}{n!} (i\omega)^n \sum_{k=1}^{p} \alpha_k^{(j)} \sum_{l=1}^{2n+1} \kappa_l^n(\boldsymbol{x})\mu_{l,k}$$

$$= \sum_{n=0}^{\infty} \frac{1}{n!} (i\omega)^n \sum_{l=1}^{2n+1} \kappa_l^n(\boldsymbol{x}) \sum_{k=1}^{p} \alpha_k^{(j)} \mu_{l,k} \, ,$$

and observe that, by definition of $\alpha_k^{(j)}$,

$$\sum_{k=1}^{p} \alpha_k^{(j)} \mu_{l,k} = \delta_{lj} \, , \quad 1 \le l, j \le p \, .$$

Thus, we infer

$$\sum_{k=1}^{p} \alpha_k^{(j)} e_k(\boldsymbol{x}) = \sum_{n=\left[\frac{j}{2}\right]}^{m} \frac{1}{n!} (i\omega)^n \kappa_j^n(\boldsymbol{x})$$

$$+ \sum_{n=m+1}^{\infty} \frac{1}{n!} (i\omega)^n \left(\kappa_j^n(\boldsymbol{x}) + \sum_{l=p+1}^{2n+1} \kappa_l^n(\boldsymbol{x}) \sum_{k=1}^{p} \alpha_k^{(j)} \mu_{l,k} \right) \, .$$

This means

$$b_j(\boldsymbol{x}) = \sum_{n=\left[\frac{j}{2}\right]}^{m} \frac{1}{n!} (i\omega)^{n-\left[\frac{j}{2}\right]} \kappa_j^n(\boldsymbol{x}) + \omega^{m+1-\left[\frac{j}{2}\right]} R_j(\omega, \boldsymbol{x}) \, , \tag{4.14}$$

with a remainder function $R_j(\omega, \boldsymbol{x})$ that, thanks to $|\kappa_j^n(\boldsymbol{x})| \leq 2|\boldsymbol{x}|^n$, is uniformly bounded on compact sets. This immediately gives

$$\lim_{\omega \to 0} b_j(\boldsymbol{x}) = \frac{1}{\left[\frac{j}{2}\right]!} \kappa_j^{\left[\frac{j}{2}\right]}(\boldsymbol{x}) . \tag{4.15}$$

Unraveling the definition of κ_j^n, we find

$$\kappa_1^0 = \tfrac{1}{2}\gamma_0^0 \equiv 1 \,, \quad \kappa_j^{\left[\frac{j}{2}\right]} = \gamma_{\frac{j}{2}}^{\frac{j}{2}} \quad \text{for even } j \,, \quad \kappa_j^{\left[\frac{j}{2}\right]} = \sigma_{\frac{j-1}{2}}^{\frac{j-1}{2}} \quad \text{for odd } j \geq 3 \,.$$

This links the limits to the integrals

$$\frac{1}{\pi} \int_{-\pi}^{\pi} (x \cos\varphi + y \sin\varphi)^n \exp(in\varphi)\, \mathrm{d}\varphi = \frac{1}{\pi} \int_{-\pi}^{\pi} \frac{1}{2^n} (\exp(i\varphi)\overline{z} + \exp(-i\varphi)z)^n \exp(in\varphi)\, \mathrm{d}\varphi$$

$$= \frac{1}{2^n} z^n \,, \quad \text{with} \quad z = x + iy \,, \quad n \in \mathbb{N} \,,$$

which gives us

$$\kappa_j^{\left[\frac{j}{2}\right]}(\boldsymbol{x}) = 2^{-\left[\frac{j}{2}\right]} \left\{ \begin{array}{c} \mathrm{Re} \\ \mathrm{Im} \end{array} \right\} (x + iy)^{\left[\frac{j}{2}\right]} \,, \quad \left\{ \begin{array}{l} \text{for even } j \,, \\ \text{for odd } j \,. \end{array} \right. \tag{4.16}$$

So the basis functions b_j tend to scaled standard harmonic polynomials in the limit $\omega \to 0$:

$$\left\{ b_j^0(\boldsymbol{x}) := \lim_{\omega \to 0} b_j(\boldsymbol{x}) \right\}_{j=1}^{p} = \left\{ 1, \frac{2^{-k}}{k!} \mathrm{Re}(x + iy)^k, \frac{2^{-k}}{k!} \mathrm{Im}(x + iy)^k \right\}_{k=1}^{m} . \tag{4.17}$$

Those are, of course, linearly independent. Thus, we retain linear independence of the functions in the limit $\omega \to 0$.

REMARK 4.3. *The use of odd p is essential, in fact, with even p, one would end up with an incomplete space of harmonic polynomials in the limit $\omega \to 0$; see (4.17). Moreover, for even p, the matrix $\boldsymbol{M}_p$ from (4.5) can be singular (take, e.g., $p = 2$, $0 < \varphi_1 < 2\pi$ and $\varphi_2 = 2\pi - \varphi_1$) and the definition of the stable basis functions is no longer valid.*

Now, we take for granted that the directions $\boldsymbol{d}_j$ are uniformly spaced on the circle, that is,

$$\boldsymbol{d}_j = \begin{pmatrix} \cos(\frac{2\pi}{p}(j-1) + \xi) \\ \sin(\frac{2\pi}{p}(j-1) + \xi) \end{pmatrix} \,, \quad j = 1, \ldots, p, \quad \xi \in \mathbb{R} \,. \tag{4.18}$$

This is the customary choice, which is also made in the standard ultra weak discontinuous Galerkin formulation. The special plane wave space distinguished by equispaced directions (4.18) will be designated by $PW_\omega^{p,\xi}(\mathbb{R}^2)$.

LEMMA 4.4. *For the particular choice $\varphi_j = \frac{2\pi}{p}(j-1) + \xi$, $j = 1, \ldots, p$, $\xi \in \mathbb{R}$, the matrix $\boldsymbol{M}_p$ from (4.5) satisfies $\boldsymbol{M}_p \boldsymbol{M}_p^H = \mathrm{diag}(p, \frac{1}{2}p, \ldots, \frac{1}{2}p)$.*

Proof. We only need to consider the case $\xi = 0$ (the result for $\xi \neq 0$ will follow in a straightforward way). For the the first row and column, it holds

$$\left(\boldsymbol{M}_p \boldsymbol{M}_p^H\right)_{1,s} = \left(\boldsymbol{M}_p \boldsymbol{M}_p^H\right)_{s,1} = \begin{cases} p & \text{for } s = 1 \,, \\ \sum_{j=1}^{p} \cos(\frac{s}{2}\varphi_j) & \text{for even } s \,, \\ \sum_{j=1}^{p} \sin(\frac{s-1}{2}\varphi_j) & \text{for odd } s \geq 3 \,. \end{cases}$$

For even s, we have

$$\sum_{j=1}^{p} \cos(\tfrac{s}{2}\varphi_j) = \sum_{k=0}^{p-1} \cos\left(\tfrac{s}{2}\,\tfrac{2\pi k}{p}\right) = \frac{1}{2}\left[\sum_{k=0}^{p-1} \exp\left(i\,\tfrac{s\pi}{p}\right)^k + \sum_{k=0}^{p-1} \exp\left(-i\,\tfrac{s\pi}{p}\right)^k\right]$$

$$= \frac{1}{2}\left[\frac{1-\exp\left(i\,\tfrac{s\pi}{p}\right)^p}{1-\exp\left(i\,\tfrac{s\pi}{p}\right)} + \frac{1-\exp\left(-i\,\tfrac{s\pi}{p}\right)^p}{1-\exp\left(-i\,\tfrac{s\pi}{p}\right)}\right] = 0.$$

For odd $s \geq 3$, the identity $\sum_{j=1}^{p} \sin(\tfrac{s-1}{2}\varphi_j) = 0$ can be obtained in a similar way; then the first row and column are $[p, 0, \ldots, 0]$. Using similar arguments, we also obtain

$$\text{for even } s, t: \quad \sum_{j=1}^{p} \cos(\tfrac{s}{2}\varphi_j)\cos(\tfrac{t}{2}\varphi_j) = \tfrac{1}{2}p\,\delta_{s,t}\,,$$

$$\text{for odd } s, t \geq 3: \quad \sum_{j=1}^{p} \sin(\tfrac{s-1}{2}\varphi_j)\sin(\tfrac{t-1}{2}\varphi_j) = \tfrac{1}{2}p\,\delta_{s,t}\,,$$

$$\text{for even } s, \text{ odd } t \geq 3: \quad \sum_{j=1}^{p} \cos(\tfrac{s}{2}\varphi_j)\sin(\tfrac{t-1}{2}\varphi_j) = 0\,;$$

consequently, for $2 \leq s, t \leq p$, $\left(\boldsymbol{M}_p\boldsymbol{M}_p^H\right)_{s,t} = \tfrac{1}{2}p\,\delta_{s,t}$, and the proof is complete. $\square$

In concrete terms, the result of Lemma 4.4 means

$$b_j(\boldsymbol{x}) = \begin{cases} \frac{1}{p}\sum_{k=1}^{p} e_k(\boldsymbol{x}) & \text{for } j = 1\,, \\[2mm] (i\omega)^{-\frac{j}{2}}\frac{2}{p}\sum_{k=1}^{p}\cos(\tfrac{j}{2}\varphi_k)e_k(\boldsymbol{x}) & \text{for even } j\,, \\[2mm] (i\omega)^{-\frac{j-1}{2}}\frac{2}{p}\sum_{k=1}^{p}\sin(\tfrac{j-1}{2}\varphi_k)e_k(\boldsymbol{x}) & \text{for odd } j \geq 3\,. \end{cases} \qquad (4.19)$$

REMARK 4.5. *Use of the stable basis $\{b_j\}_{j=1}^{p}$ is essential in numerical studies of low-wavenumber asymptotics. Yet, the representation (4.19) is prone to cancellation and useless in numerical terms. Instead, we use the series expansion (4.14) up to ω^{13}. The resulting truncation errors are illustrated in Figure 4.1: for large ω the truncation error becomes large, for small ω the instability of the exponential basis makes the (MATLAB) computation sensitive to roundoff. For $\frac{1}{2} \leq \omega \leq 1$, $\boldsymbol{x} \in K$, and $p \leq 11$ the resulting truncation errors are below 10^{-5} uniformly.*

REMARK 4.6. *The construction of a stable basis is closely linked to plane wave representation formulas for circular wave Helmholtz solutions*

$$\boldsymbol{x} \mapsto \omega^{-n}J_n(\omega r)\exp(\pm in\theta)\,, \quad \boldsymbol{x} = \begin{pmatrix} r\cos\theta \\ r\sin\theta \end{pmatrix}\,, \quad n \in \mathbb{N}_0\,, \qquad (4.20)$$

where J_n is a Bessel function. For those we have the integral representation

$$J_n(z) = \frac{(-1)^n}{2\pi}\int_0^{2\pi} \exp(iz\cos\varphi)e^{in\varphi}\,\mathrm{d}\varphi\,, \quad z \in \mathbb{C}, n \in \mathbb{N}_0\,. \qquad (4.21)$$

From the series expansion

$$J_n(z) = \left(\frac{z}{2}\right)^n \sum_{l=0}^{\infty} \frac{1}{l!(n+l)!}\left(-\frac{z^2}{4}\right)^l\,, \quad z \in \mathbb{C}\,, \qquad (4.22)$$
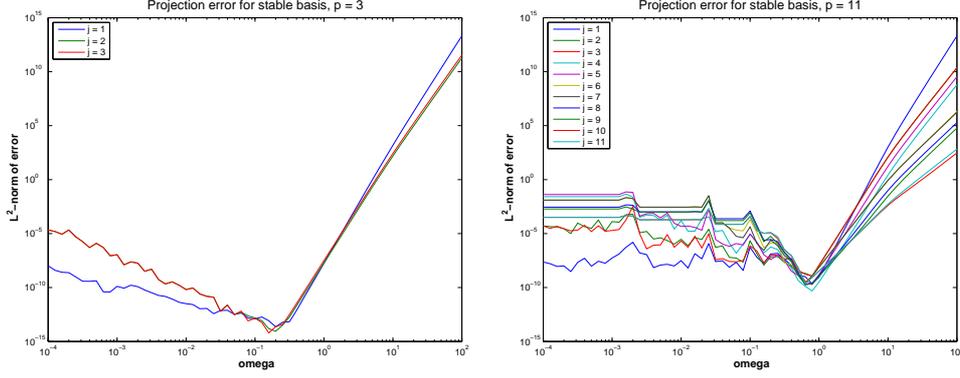
FIG. 4.1. *Residual norm for L^2 projection of truncated basis functions b_j onto plane wave space. Truncation after 13 terms in the expansion w.r.t. ω.*

it becomes clear that, in the limit $\omega \to 0$, the span of the functions, written in polar coordinates (r, θ),

$$\left\{ J_0(\omega r), \operatorname{Re} \frac{J_1(\omega r)}{\omega} e^{i\theta}, \operatorname{Im} \frac{J_1(\omega r)}{\omega} e^{i\theta}, \ldots, \operatorname{Re} \frac{J_m(\omega r)}{\omega^m} e^{im\theta}, \operatorname{Im} \frac{J_m(\omega r)}{\omega^m} e^{im\theta} \right\} \quad (4.23)$$

will be the same as that of the harmonic polynomials in (4.17). This suggests a relationship to the stable basis functions b_j from (4.6):

$$b_1 \sim J_0(\omega r), \quad b_j \sim \begin{cases} \omega^{-\frac{j}{2}} \operatorname{Re} J_{\frac{j}{2}}(\omega r) e^{i\frac{j}{2}\theta} & \text{for even } j, \\ \omega^{-\frac{j-1}{2}} \operatorname{Im} J_{\frac{j-1}{2}}(\omega r) e^{i\frac{j-1}{2}\theta} & \text{for odd } j. \end{cases} \quad (4.24)$$

Using (4.21) we can rewrite

$$J_n(\omega r) e^{in\theta} = \frac{(-1)^n}{2\pi} \int_0^{2\pi} \exp(in\varphi) \exp\left(i\omega \begin{pmatrix} \cos\varphi \\ \sin\varphi \end{pmatrix} \cdot \boldsymbol{x} \right) \, d\varphi. \quad (4.25)$$

The integral can be approximated by the p-point trapezoidal rule, $p = 2m + 1$. In combination with (4.24) this yields

$$b_1(\boldsymbol{x}) \sim \frac{1}{p} \sum_{l=1}^p \exp(i\omega \boldsymbol{d}_l \cdot \boldsymbol{x}),$$

$$b_j(\boldsymbol{x}) \sim \begin{cases} \omega^{-\frac{j}{2}} \frac{1}{p} \sum_{l=1}^p \cos(\frac{j}{2}\varphi_l) e_l(\boldsymbol{x}) & \text{for even } j, \\ \omega^{-\frac{j-1}{2}} \frac{1}{p} \sum_{l=1}^p \sin(\frac{j-1}{2}\varphi_l) e_l(\boldsymbol{x}) & \text{for odd } j, \end{cases}$$

with $\boldsymbol{d}_l$ introduced in (4.18), φ_l defined in Lemma 4.4. Up to scaling this agrees with (4.19).

Some theoretical investigations will also rely on the augmented space

$$\begin{aligned} PPW_\omega(\mathbb{R}^2) &:= PW_\omega(\mathbb{R}^2) + \mathcal{P}_1(\mathbb{R}^2) \\ &= \langle 1, i\omega x, i\omega y, \exp(i\omega \boldsymbol{d}_1 \cdot \boldsymbol{x}), \ldots, \exp(i\omega \boldsymbol{d}_p \cdot \boldsymbol{x}) \rangle, \end{aligned} \quad (4.26)$$

where $\mathcal{P}_1(\mathbb{R}^2)$ designates the space of two-variate affine linear functions.

For theoretical and computational purposes we also need a basis of $PPW_\omega(\mathbb{R}^2)$ that remains stable for $\omega \to 0$. First we modify the plane wave functions e_k by subtracting the linear parts

$$\widetilde{e}_k(\boldsymbol{x}) := \exp(i\omega\boldsymbol{d}_k \cdot \boldsymbol{x}) - 1 - i\omega\boldsymbol{d}_k \cdot \boldsymbol{x} . \tag{4.27}$$

It goes without saying that $\langle 1, i\omega x, i\omega y, \widetilde{e}_1, \ldots, \widetilde{e}_p \rangle$ still constitutes a basis of $PPW_\omega(\mathbb{R}^2)$. This time we define $\alpha_k^{(j)}$, $1 \le k, j \le p$, $p \ge 5$, by

$$\left(\sum_{k=1}^p \alpha_k^{(j)} \mu_{l,k} \right)_{j,l=1}^p = \left(\rho_l^{(j)} \right)_{j,l=1}^p := \begin{pmatrix} 1 & 0 & 0 & 0 & 0 & 0 & \cdots & \cdots & 0 \\ 0 & 0 & 0 & 1 & 0 & 0 & & & \vdots \\ 0 & 0 & 0 & 0 & 1 & 0 & & & \\ 0 & 1 & 0 & 0 & 0 & 0 & & & \\ 0 & 0 & 1 & 0 & 0 & 0 & & & \\ 0 & 0 & 0 & 0 & 0 & 1 & \ddots & & \\ \vdots & & & & & & \ddots & 1 & \ddots & \vdots \\ \vdots & & & & & & & \ddots & \ddots & 0 \\ 0 & \cdots & & & & & \cdots & 0 & 1 \end{pmatrix} . \tag{4.28}$$

Thanks to Lemma 4.2, this is a valid definition . The coefficients $\alpha_k^{(j)}$ can be used to define the new basis functions. To justify this, we use the exponential series and (4.13) to write, with $\rho_l^{(j)}$ defined in (4.28),

$$\begin{aligned}
\sum_{k=1}^p \alpha_k^{(j)} \widetilde{e}_k &= \sum_{k=1}^p \alpha_k^{(j)} \sum_{n=2}^\infty \frac{1}{n!}(i\omega)^n \left(\begin{pmatrix} \cos\varphi_k \\ \sin\varphi_k \end{pmatrix} \cdot \boldsymbol{x} \right)^n \\
&= \sum_{n=2}^\infty \frac{1}{n!}(i\omega)^n \sum_{l=1}^{2n+1} \kappa_l^n(\boldsymbol{x}) \sum_{k=1}^p \alpha_k^{(j)} \mu_{l,k} \\
&= \sum_{n=2}^m \frac{1}{n!}(i\omega)^n \sum_{l=1}^{2n+1} \rho_l^{(j)} \kappa_l^n(\boldsymbol{x}) + \sum_{n=m+1}^\infty \frac{1}{n!}(i\omega)^n \sum_{l=1}^{2n+1} \kappa_l^n(\boldsymbol{x}) \sum_{k=1}^p \alpha_k^{(j)} \mu_{l,k} \\
&= \sum_{n=2}^m \frac{1}{n!}(i\omega)^n \sum_{l=1}^{2n+1} \rho_l^{(j)} \kappa_l^n(\boldsymbol{x}) + (i\omega)^{m+1} R_j(\omega, \boldsymbol{x}) ,
\end{aligned} \tag{4.29}$$

where the remainder term is uniformly bounded on $\mathbb{R} \times [0,1]^2$. Thus, for $p \ge 5$, we

define special basis functions

$$b_1 := (i\omega)^{-2} \sum_{k=1}^{p} \alpha_k^{(1)} \widetilde{e}_k \quad \Rightarrow \lim_{\omega \to 0} b_1(\boldsymbol{x}) = \tfrac{1}{2}\kappa_1^2(\boldsymbol{x}) = \tfrac{1}{4}(x^2 + y^2) \,, \qquad (4.30)$$

$$b_2 := (i\omega)^{-2} \sum_{k=1}^{p} \alpha_k^{(2)} \widetilde{e}_k \quad \Rightarrow \lim_{\omega \to 0} b_2(\boldsymbol{x}) = \tfrac{1}{2}\kappa_4^2(\boldsymbol{x}) = \tfrac{1}{4}(x^2 - y^2) \,, \qquad (4.31)$$

$$b_3 := (i\omega)^{-2} \sum_{k=1}^{p} \alpha_k^{(3)} \widetilde{e}_k \quad \Rightarrow \lim_{\omega \to 0} b_3(\boldsymbol{x}) = \tfrac{1}{2}\kappa_5^2(\boldsymbol{x}) = \tfrac{1}{2}xy \,, \qquad (4.32)$$

$$b_4 := (i\omega)^{-3} \sum_{k=1}^{p} \alpha_k^{(4)} \widetilde{e}_k \quad \Rightarrow \lim_{\omega \to 0} b_4(\boldsymbol{x}) = \tfrac{1}{6}\kappa_2^3(\boldsymbol{x}) = \tfrac{1}{24}(x^3 + 3xy^2) \,, \qquad (4.33)$$

$$b_5 := (i\omega)^{-3} \sum_{k=1}^{p} \alpha_k^{(5)} \widetilde{e}_k \quad \Rightarrow \lim_{\omega \to 0} b_5(\boldsymbol{x}) = \tfrac{1}{6}\kappa_3^3(\boldsymbol{x}) = \tfrac{1}{24}(y^3 + 3yx^2) \,. \qquad (4.34)$$

We conclude the limits from (4.29), the definition of $\rho_l^{(j)}$ in (4.28) and the fact that, *cf.* (4.12),

$$\kappa_l^2 = 0 \quad \text{for } l \notin \{1, 4, 5\} \,, \quad \kappa_l^3 = 0 \quad \text{for } l \notin \{2, 3, 6, 7\} \,. \qquad (4.35)$$

For the remaining basis functions b_j, $j = 6, \ldots, p$, we resort to the usual formula, *cf.* (4.6),

$$b_j := (i\omega)^{-\left[\frac{j}{2}\right]} \sum_{k=1}^{p} \alpha_k^{(j)} \widetilde{e}_k \,, \qquad (4.36)$$

and recover the limit (4.15). For $p \geq 7$, we point out that we have

$$b_6 := (i\omega)^{-3} \sum_{k=1}^{p} \alpha_k^{(6)} \widetilde{e}_k \quad \Rightarrow \lim_{\omega \to 0} b_6(\boldsymbol{x}) = \tfrac{1}{6}\kappa_6^3(\boldsymbol{x}) = \tfrac{1}{48}(x^3 - 3xy^2) \,, \qquad (4.37)$$

$$b_7 := (i\omega)^{-3} \sum_{k=1}^{p} \alpha_k^{(7)} \widetilde{e}_k \quad \Rightarrow \lim_{\omega \to 0} b_8(\boldsymbol{x}) = \tfrac{1}{6}\kappa_7^3(\boldsymbol{x}) = \tfrac{1}{48}(-y^3 + 3yx^2) \,. \qquad (4.38)$$

Summing up,
- if $p \geq 3$, for $\omega \to 0$ the functions in the set $\{1, x, y, b_1, b_2, b_3\}$ will uniformly converge to a stable polynomial basis of the full space $\mathcal{P}_2(\mathbb{R}^2)$ of quadratic bi-variate polynomials,
- if $p \geq 7$, the functions in $\{1, x, y, b_k\}_{k=1}^{7}$ have $\boldsymbol{x}$–uniform limits for $\omega \to 0$ and converge to a basis of $\mathcal{P}_3(\mathbb{R}^2)$.
- the limits $\lim_{\omega \to 0} b_j$, $j \geq 6$, provide linearly independent harmonic polynomials of degree $[\frac{j}{2}]$, see (4.17).

Thus we have found a basis of $PPW_\omega(\mathbb{R}^2)$ that does not degenerate as $\omega \to 0$.

Again, we examine the stable basis for the special case of equispaced directions

(4.18). Using Lemma 4.4, the defining equations (4.28) imply, for $p \geq 5$,

$$\left(\alpha_k^{(j)}\right)_{j,k=1}^p = \mathrm{diag}(\frac{1}{p}, \frac{2}{p}, \ldots, \frac{2}{p}) \boldsymbol{M}_p \left(\begin{array}{c|c} \begin{pmatrix} 1 & 0 & 0 & 0 & 0 \\ 0 & 0 & 0 & 1 & 0 \\ 0 & 0 & 0 & 0 & 1 \\ 0 & 1 & 0 & 0 & 0 \\ 0 & 0 & 1 & 0 & 0 \end{pmatrix} & \boldsymbol{0} \\ \hline \boldsymbol{0} & \boldsymbol{I} \end{array} \right), \qquad (4.39)$$

where $\boldsymbol{I}$ denotes the $(p-5) \times (p-5)$-identity matrix. In terms of basis functions this means, for $p \geq 5$,

$$b_j = \begin{cases} (i\omega)^{-2} \frac{1}{p} \sum_{k=1}^p \widetilde{e}_k & \text{for } j = 1 , \\[2mm] (i\omega)^{-2} \frac{2}{p} \sum_{k=1}^p \cos(2\varphi_k)\widetilde{e}_k & \text{for } j = 2 , \\[2mm] (i\omega)^{-2} \frac{2}{p} \sum_{k=1}^p \sin(2\varphi_k)\widetilde{e}_k & \text{for } j = 3 , \\[2mm] (i\omega)^{-3} \frac{2}{p} \sum_{k=1}^p \cos(\varphi_k)\widetilde{e}_k & \text{for } j = 4 , \\[2mm] (i\omega)^{-3} \frac{2}{p} \sum_{k=1}^p \sin(\varphi_k)\widetilde{e}_k & \text{for } j = 5 , \\[2mm] (i\omega)^{-\frac{j}{2}} \frac{2}{p} \sum_{k=1}^p \cos(\frac{j}{2}\varphi_k)\widetilde{e}_k & \text{for even } j > 5 , \text{ if } p \geq 7 , \\[2mm] (i\omega)^{-\frac{j-1}{2}} \frac{2}{p} \sum_{k=1}^p \sin(\frac{j-1}{2}\varphi_k)\widetilde{e}_k & \text{for odd } j > 5 , \text{ if } p \geq 7 . \end{cases} \qquad (4.40)$$

4.2. Inverse and projection estimates for plane waves. In order to develop a convergence theory for the h–version of the DG methods from Section 3 with plane wave trial and test functions, we aim to establish element-by-element inverse and projection estimates for $PW_\omega^{p,\xi}(\mathbb{R}^2)$ that parallel those for piecewise polynomials. As usual we have to limit the distortion of the triangles.

ASSUMPTION 4.6.1 (Shape regularity). *All angles of triangles in $\mathcal{T}_h$ are bounded from below by $\alpha_0 > 0$.*

Our analysis heavily relies on *scaling techniques* employing similarity mappings $\boldsymbol{\Phi}_K$, that is, compositions of rigid motions and scalings:

$$\boldsymbol{\Phi}_K : \widehat{K} \mapsto K , \quad \boldsymbol{\Phi}_K(\widehat{\boldsymbol{x}}) = \tfrac{h_K}{h_{\widehat{K}}} \mathbf{Q}\widehat{\boldsymbol{x}} + \boldsymbol{t}, \ \mathbf{Q}^T = \mathbf{Q}^{-1}, \ \boldsymbol{t} \in \mathbb{R}^2 . \qquad (4.41)$$

A function $v \in PW_\omega^{p,0}(K)$ pulled back to $\widehat{K}$ has the representation

$$(v \circ \boldsymbol{\Phi}_K)(\widehat{\boldsymbol{x}}) =: \widehat{v}(\widehat{\boldsymbol{x}}) = \sum_{j=1}^p \alpha_j \exp(i\,\tfrac{h_K}{h_{\widehat{K}}}\,\omega \widehat{\boldsymbol{d}}_j \cdot \widehat{\boldsymbol{x}}) , \quad \alpha_j \in \mathbb{C}, \ \widehat{\boldsymbol{x}} \in \widehat{K} , \qquad (4.42)$$

with, by (4.18),

$$\widehat{\boldsymbol{d}}_j = \begin{pmatrix} \cos(\frac{2\pi}{p}(j-1) + \gamma) \\ \sin(\frac{2\pi}{p}(j-1) + \gamma) \end{pmatrix} , \quad j = 1, \ldots, p , \quad \gamma \in \mathbb{R} . \qquad (4.43)$$

The angle γ reflects the rotation $\mathbf{Q}$ involved in the mapping to $\widehat{K}$. In short, the image of $PW_\omega^{p,0}(\mathbb{R}^2)$ under similarity pullback is $PW_{\widehat{\omega}}^{p,\gamma}(\mathbb{R}^2)$, $\widehat{\omega} := \frac{h_K}{h_{\widehat{K}}} \omega$. It is essential to note that even if two triangles are mapped to the same "reference triangle" $\widehat{K}$, the

mapped plane wave spaces will not necessarily agree. This foils standard finite element Bramble-Hilbert type arguments, see [6, Sect. 4.3.8].

The first class of inequalities are trace inverse estimates connecting norms of traces onto element boundaries with norms over the element itself.

THEOREM 4.7. *Let Assumption 4.6.1 hold and p be odd. Then there exists a constant $C_{\mathrm{tinv}} > 0$ such that*

$$\|v\|_{0,\partial K} \le C_{\mathrm{tinv}} h_K^{-1/2} \|v\|_{0,K} \qquad \forall v \in PW_\omega^{p,0}(\mathbb{R}^2), \ \forall K \in \mathcal{T}_h, \ \forall \omega \ge 0 \ .$$

Proof. (i) Pick any $K \in \mathcal{T}_h$ and an edge $e \subset \partial K$. There is a unique similarity mapping $\boldsymbol{\Phi}_K$ according to (4.41) such that the line segment $\widehat{e} = \left[\binom{-1}{0}, \binom{1}{0}\right]$ is mapped onto e. Write $\widehat{K}$ for the pre-image of K under $\boldsymbol{\Phi}_K$. If we can establish the existence of $C > 0$ that may only depend on α_0 from Assumption 4.6.1, such that

$$\|v\|_{0,\widehat{e}} \le C \|v\|_{0,\widehat{K}} \quad \forall v \in PW_{\widehat{\omega}}^{p,\gamma}(\mathbb{R}^2), \ \forall \gamma \in [0, 2\pi[, \ \forall \widehat{\omega} \in \mathbb{R}^+ \ , \tag{4.44}$$

then the assertion of the theorem will follow by simple scaling arguments. Assumption 4.6.1 also guarantees that the isosceles triangle T with base $\widehat{e}$ and base angle α_0 is contained in $\widehat{K}$. Thus, (4.44) is already implied by

$$\exists C > 0: \quad \|v\|_{0,\widehat{e}} \le C \|v\|_{0,T} \quad \forall v \in PW_{\widehat{\omega}}^{p,\gamma}(\mathbb{R}^2), \ \forall \gamma \in [0, 2\pi[, \ \forall \widehat{\omega} \in \mathbb{R}^+ \ . \tag{4.45}$$

(ii) If we choose some basis $\{w_j\}_{j=1}^p$ of $PW_{\widehat{\omega}}^{p,\gamma}(\mathbb{R}^2)$, the computation of the best possible value for C from (4.45) can be converted into a generalized eigenvalue problem for matrices: this C agrees with the square root of the largest eigenvalue $\lambda_{\max} = \lambda_{\max}(\widehat{\omega}, \gamma)$ of the generalized eigenvalue problem

$$\lambda \in \mathbb{R}, \ \vec{\alpha} \in \mathbb{R}^p \setminus \{0\}: \quad \boldsymbol{T}\vec{\alpha} = \lambda \boldsymbol{M}\vec{\alpha} \ , \tag{4.46}$$

with the mass matrices

$$\boldsymbol{T} := \left(\int_{\widehat{e}} w_k(\boldsymbol{x}) \cdot \overline{w}_j(\boldsymbol{x}) \, \mathrm{d}S \right)_{1 \le k,j \le p} \ , \quad \boldsymbol{M} := \left(\int_T w_k(\boldsymbol{x}) \cdot \overline{w}_j(\boldsymbol{x}) \, \mathrm{d}\boldsymbol{x} \right)_{1 \le k,j \le p} \ .$$

The eigenvalues of (4.46) do not depend on the choice of basis. Guided by convenience, we may therefore either choose the stable basis $\{b_j\}_{j=1}^p$ from (4.19) or the standard basis $\{e_j\}_{j=1}^p$, see Lemma 4.1.

(iii) No matter which basis is used, both Hermitian $p \times p$–matrices $\boldsymbol{T}$ and $\boldsymbol{M}$ are analytic functions of $\widehat{\omega} \in \mathbb{R}^+$, $\gamma \in [0, 2\pi]$. Moreover, linear independence of the plane waves renders $\boldsymbol{M}$ positive definite for $\widehat{\omega} \ne 0$. Hence, the eigenvalues will be analytic functions of $\widehat{\omega}$ and γ on $\mathbb{R}^+ \times [0, 2\pi]$ (and periodic in γ).

For small ω, the basis $\{b_j\}_{j=1}^p$ is convenient. The uniform convergence of the b_j for $\widehat{\omega} \to 0$ carries over to the mass matrices. Both $\boldsymbol{T}$ and $\boldsymbol{M}$ enjoy a uniform limit for $\widehat{\omega} \to 0$, which agrees with the mass matrices $\boldsymbol{T}^0$, $\boldsymbol{M}^0$ arising from the use of the harmonic polynomial basis $\{b_j^0\}_{j=1}^p$, see (4.17). Obviously, $\boldsymbol{M}^0$ is positive definite, and $\boldsymbol{T}^0$ does not vanish. Hence, the eigenvalues from (4.46) (as functions of $\widehat{\omega}$) have a continuous extension to $\widehat{\omega} = 0$. Note that the limit does not depend on γ.

We conclude, that $\lambda_{\max}(\widehat{\omega}, \gamma)$ can be extended to $\widehat{\omega} = 0$ with a positive value $\lambda_{\max}(0, \gamma) = \lambda_{\max}(0) > 0$ (independent of γ). Thus, $\lambda_{\max}$ turns out to be a positive and continuous function on $\mathbb{R}_0^+ \times [0, 2\pi]$.

(iv) To determine the behavior of $\lambda_{\max}(\widehat{\omega}, \gamma)$ for $\widehat{\omega} \to \infty$, we resort to the standard basis given in Lemma 4.1. Then, writing $\delta x_{jk} := d_{j,1} - d_{k,1}$, $\delta y_{jk} := d_{j,2} - d_{k,2}$, $a := \tan(\alpha_0)$, we find

$$(\boldsymbol{T})_{jk} = 2\operatorname{sinc}(i\widehat{\omega}\delta x_{jk}) , \quad 1 \le k, j \le p , \tag{4.47}$$

$$(\boldsymbol{M})_{jk} = \int\limits_{0}^{a} \int\limits_{-1+y/a}^{1-y/a} \exp(i\widehat{\omega}(\delta x_{jk}x + \delta y_{jk}y))\, \mathrm{d}x\mathrm{d}y , \quad 1 \le k, j \le p . \tag{4.48}$$

Obviously, the Euclidean matrix norm of $\boldsymbol{T}$ can be bounded by $\|\boldsymbol{T}\| \le 2p$. Further, $\boldsymbol{M}_{jj} = a$ for $1 \le j \le p$. To estimate the off-diagonal matrix entries $(\boldsymbol{M})_{jk}$, $k \ne j$, we use $|\boldsymbol{d}_j - \boldsymbol{d}_k|^2 = \delta x_{kj}^2 + \delta y_{kj}^2 = 4\sin^2(\frac{\pi}{p}|k - j|)$ and distinguish two cases.

(i) If $|\delta x_{jk}| \ge |\delta y_{jk}|$, we infer $|\delta x_{jk}| \ge \sin(\frac{\pi}{p}|k - j|) > 0$. Thus, we can directly evaluate the inner integral of (4.48)

$$(\boldsymbol{M})_{jk} = 2\int\limits_{0}^{a} \exp(i\widehat{\omega}\delta y_{jk}y)(1 - y/a)\operatorname{sinc}(\widehat{\omega}\delta x_{jk}(1 - y/a))\, \mathrm{d}y$$

$$\le 2a\int\limits_{0}^{1} \min\{1 - y, \frac{1}{\widehat{\omega}\delta x_{jk}}\}\, \mathrm{d}y = \frac{a}{\widehat{\omega}\delta x_{jk}}\left(1 + \frac{1}{\widehat{\omega}\delta x_{jk}} - \frac{1}{(\widehat{\omega}\delta x_{jk})^2}\right) .$$

This expression tends to zero uniformly as $\widehat{\omega} \to \infty$.

(ii) In the case $|\delta x_{jk}| < |\delta y_{jk}|$, that is, $|\delta y_{jk}| > \sin(\frac{\pi}{p}|k - j|) > 0$, we change the order of integration in (4.48) and obtain

$$(\boldsymbol{M})_{jk} = 2\int\limits_{0}^{1} \cos(\widehat{\omega}\delta x_{jk}x)\frac{\exp(i\widehat{\omega}\delta y_{jk}a(1 - x)) - 1}{i\widehat{\omega}\delta y_{jk}}\, \mathrm{d}x$$

$$\le 4\int\limits_{0}^{1} \min\{a(1 - x), \frac{1}{\widehat{\omega}\delta y_{jk}}\}\, \mathrm{d}y \to 0 \text{ uniformly as } \widehat{\omega} \to \infty .$$

Summing up, we found the asymptotic behavior

$$\max_{\substack{1 \le i, j \le p \\ j \ne k}} (\boldsymbol{M})_{i,j} = O(\widehat{\omega}^{-1}) \quad \text{for } \widehat{\omega} \to \infty . \tag{4.49}$$

As a consequence, for $\widehat{\omega}$ large enough, Gershgorin's theorem tells us that the smallest eigenvalue of $\boldsymbol{M}$ can be bounded from below by $\frac{1}{2}a$. We immediately infer

$$\lim_{\widehat{\omega} \to \infty} \lambda_{\max}(\widehat{\omega}, \gamma) \le \lim_{\widehat{\omega} \to \infty} \lambda_{\min}(\boldsymbol{M})^{-1}\|\boldsymbol{T}\| \le \frac{4p}{a} \qquad \forall \gamma \in [0, 2\pi[. \tag{4.50}$$

Summing up, $\lambda_{\max}(\widehat{\omega}, \gamma)$ is bounded on $\mathbb{R}_0^+ \times [0, 2\pi]$, which ensures the existence of a $C_{\text{tinv}} > 0$ in (4.45). $\square$

Numerical experiment. We have computed the constant in the inverse estimate of Theorem 4.7 numerically for the unit square $K =]0, 1[^2$ and the "unit triangle" $K := \{\boldsymbol{x} \in \mathbb{R}^2 : x_1, x_2 > 0, x_1 + x_2 < 1\}$, see Figs. 4.2 and 4.3. In addition, the shape of the triangle $K := \{\boldsymbol{x} \in \mathbb{R}^2 : x_1, x_2 > 0, ax_1 + x_2 < a\}$ is varied smoothly

in Figure 4.4. The computation were carried out in MATLAB using the standard exponential basis $\{e_k\}$ of PW_ω for $\omega \geq \frac{1}{2}$. For smaller ω the computations employed the first 13 terms in the Taylor expansions (w.r.t. ω) of the stable basis functions b_j from (4.6).
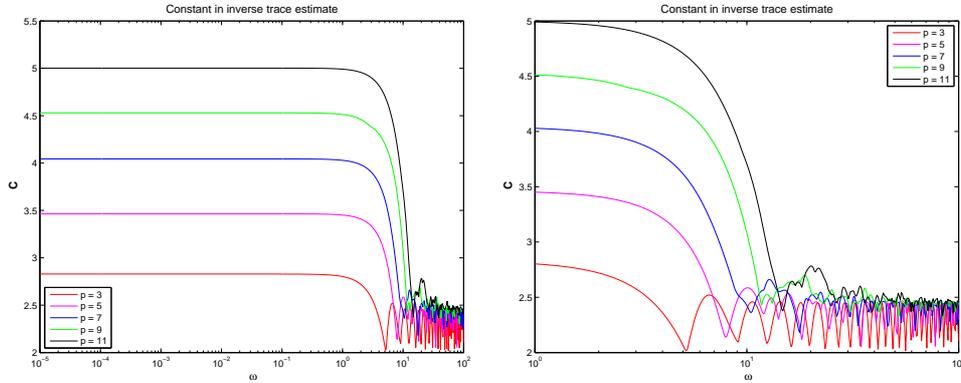

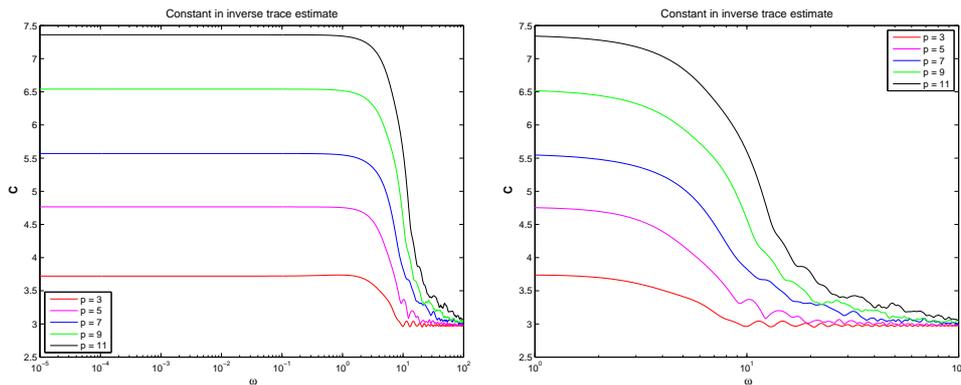FIG. 4.2. *Constants in the inverse trace norm inequality of Theorem 4.7 for $K =]0, 1[^2$*

FIG. 4.3. *Constants in the inverse trace norm inequality of Theorem 4.7 for the unit triangle*

The plots strikingly illustrate the uniform boundedness of the constant in the inverse trace inequality with respect to ω. Smooth dependence on the geometry of K is also apparent. The bound for the constants is moderate, but seems to increase linearly with p. Remember that this is also true for multivariate polynomials of degree p; see, e.g., [24, Theorem 4.76].

THEOREM 4.8. *There exists a constant $C_{\mathrm{inv}} > 0$ only depending on p and α_0 such that*

$$\|\nabla v\|_{0,K} \leq C_{\mathrm{inv}}(\omega h_K + 1)\, h_K^{-1} \|v\|_{0,K} \quad \forall v \in PW_\omega^{p,0}(\mathbb{R}^2),\ \forall K \in \mathcal{T}_h,\ \forall \omega \geq 0\ .$$

Proof. Again we resort to transformation techniques and first establish the estimate for the reference triangle $\widehat{K}$. Thanks to integration by parts and Theorem 4.7 (recall that plane wave spaces are invariant with respect to forming partial deriva-
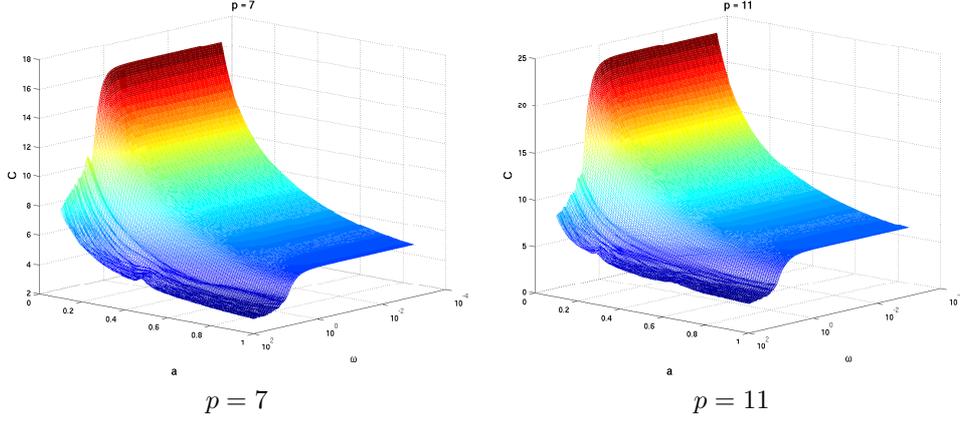
$$p = 7 \qquad\qquad\qquad p = 11$$

FIG. 4.4. *Constants in the inverse trace norm inequality for triangle with vertices $\binom{0}{0}, \binom{1}{0}, \binom{0}{a}$, $a > 0$.*

tives), we have

$$
\int_{\widehat{K}} |\nabla \widehat{v}|^2 \, \mathrm{d}\widehat{\boldsymbol{x}} = -\int_{\widehat{K}} \Delta \widehat{v} \cdot \bar{\bar{\widehat{v}}} \, \mathrm{d}\widehat{\boldsymbol{x}} + \int_{\partial \widehat{K}} \nabla \widehat{v} \cdot \widehat{\boldsymbol{n}} \, \bar{\bar{\widehat{v}}} \, \mathrm{d}\widehat{S}
$$

$$
\leq \widehat{\omega}^2 \int_{\widehat{K}} |\widehat{v}|^2 \, \mathrm{d}\widehat{\boldsymbol{x}} + \|\nabla \widehat{v}\|_{0,\partial \widehat{K}} \|\widehat{v}\|_{0,\partial \widehat{K}}
$$

$$
\leq \widehat{\omega}^2 \|\widehat{v}\|_{0,\widehat{K}}^2 + C_{\mathrm{tinv}}^2 \|\nabla \widehat{v}\|_{0,\widehat{K}} \|\widehat{v}\|_{0,\widehat{K}}
$$

$$
\leq \left(\widehat{\omega}^2 + \tfrac{1}{2} C_{\mathrm{tinv}}^4 \right) \|\widehat{v}\|_{0,\widehat{K}}^2 + \tfrac{1}{2} \|\nabla \widehat{v}\|_{0,\widehat{K}}^2 .
$$

Then transform this estimate to K. $\square$

Numerical experiment. Figs. 4.5 and 4.6 display approximate values for C_{inv} from Thm. 4.8 for the unit square $K =]0,1[^2$ and the "unit triangle" $K := \{\boldsymbol{x} \in \mathbb{R}^2 : x_1, x_2 > 0, \ x_1 + x_2 < 1\}$ ($h_K = 1$ in each case). The computations were done in MATLAB and used the truncated stable basis for $\omega \leq \frac{1}{2}$, see the previous numerical experiments.
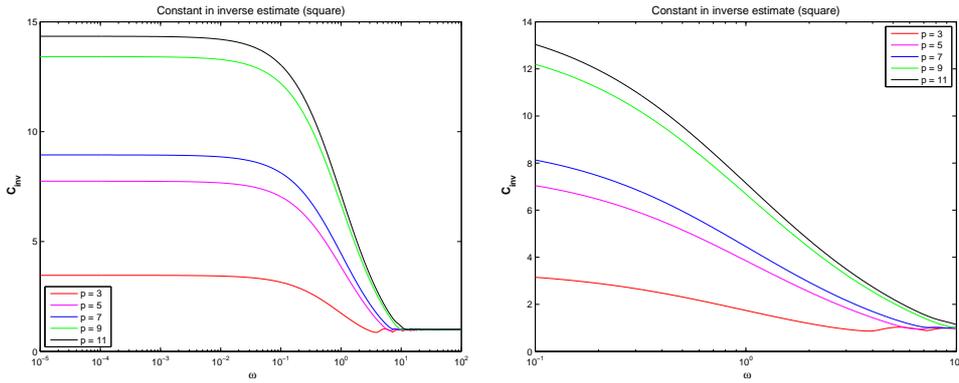

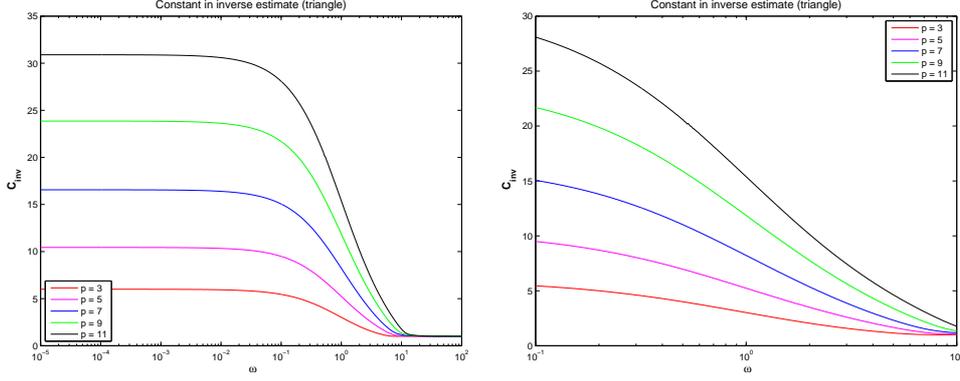FIG. 4.5. *Constant in inverse inequality of Thm. 4.8 for $K =]0,1[^2$*

FIG. 4.6. *Constant in inverse inequality of Thm. 4.8 for the unit triangle*

PROPOSITION 4.9. *The estimates of Theorem 4.7 and Theorem 4.8 still hold with* $PW_\omega^{p,\gamma}(\mathbb{R}^2)$ *replaced by* $PPW_\omega^{p,\gamma}(\mathbb{R}^2)$.

Proof. The proof can be done as above, because (4.30)–(4.34) and (4.36) give us a stable basis for $\omega \to 0$. $\square$

Next, we examine approximation and projection estimates for plane waves. We fix a triangle K that complies with Assumption 4.6.1. We study the local $L^2(K)$–orthogonal projections

$$\mathsf{P}_\omega : L^2(K) \mapsto PW_\omega^{p,\gamma}(\mathbb{R}^2) \tag{4.51}$$

onto the space of plane waves on K, see (4.18). When referring to the associated reference element $\widehat{K}$ with longest edge $\left[\binom{0}{0}, \binom{1}{0}\right]$ and the pulled back plane wave space we write $\widehat{\mathsf{P}}_{\widehat\omega}$ for this projector.

We pursue the policy to relate P_ω to the $L^2(K)$–orthogonal projection $\mathsf{Q} :$ $L^2(K) \mapsto \mathcal{P}_1(\mathbb{R}^2)$ onto the space of bi-variate polynomials of degree 1. Simple transformation techniques and Bramble-Hilbert argument establish the projection error estimates

$$\begin{aligned} \|u - \mathsf{Q}u\|_{0,K} &\le C h_K^2 |u|_{2,K} \,, \\ |u - \mathsf{Q}u|_{1,K} &\le C h_K |u|_{2,K} \end{aligned} \quad \forall u \in H^2(K) \,, \tag{4.52}$$

with $C > 0$ only depending on the minimal angle condition in Assumption 4.6.1.

The next Lemma gives a pivotal auxiliary result.

LEMMA 4.10. *For odd* $p \ge 5$ *we find* $C > 0$ *independent of* ω *and* γ *such that*

$$\inf_{v \in PW_\omega^{p,\gamma}(\mathbb{R}^2)} \|q - v\|_{0,]0,1[^2} \le C\omega^2 \|q\|_{0,]0,1[^2} \quad \forall q \in \mathcal{P}_1(\mathbb{R}^2) \,.$$

Proof. Recall (4.12), the definition of $\kappa_j^n(\boldsymbol{x})$ and the formula (4.14) for the functions of the stabilized basis. Combining them, we see that, for $p \ge 5$ and $\omega \to 0$,

$$b_1(\boldsymbol{x}) = 1 + O(\omega^2) \,, \quad b_2(\boldsymbol{x}) = x + O(\omega^2) \,, \quad b_3(\boldsymbol{x}) = y + O(\omega^2) \,,$$

for small ω uniformly in $\boldsymbol{x} \in]0,1[^2$. $\square$

REMARK 4.11. *In the case* $p = 3$ *the best approximation error for linear functions will behave like* $O(\omega)$, *because it will be affected by the remainder term in* (4.15).

Numerical experiment. We computed the error of the L^2–projection of the function $\boldsymbol{x} \mapsto x$ onto the plane wave space on $]0, 1[^2$ numerically, see Figure 4.7. As above, a truncated stable basis and the exponential basis were used for $\omega < \frac{1}{2}$ and $\omega \geq \frac{1}{2}$, respectively. This is not only in perfect agreement with Lemma 4.10, but also shows that the estimate in Lemma 4.10 is sharp and the constants are small.
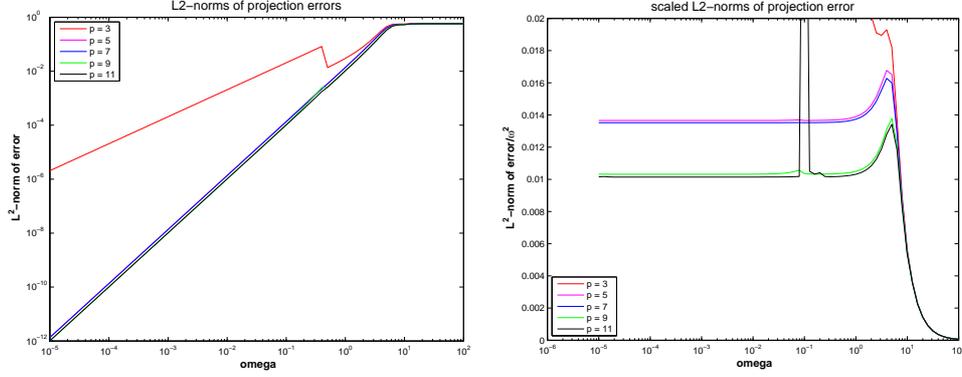

FIG. 4.7. L^2 *projection error onto plane wave space for linear function x. The wiggles at $\omega = \frac{1}{2}$ reflect the truncation error for the stable basis.*

In the next three propositions we establish projection errors and continuity of the $L^2(K)$–orthogonal projection P_ω onto $PW^{p,0}_\omega(\mathbb{R}^2)$.

PROPOSITION 4.12. *For odd $p \geq 5$ we have, with $C > 0$ independent of K and $\omega \geq 0$,*

$$\|(Id - \mathsf{P}_\omega)u\|_{0,K} \leq Ch_K^2(|u|_{2,K} + \omega^2\|u\|_{0,K}) \quad \forall u \in H^2(K) .$$

Proof. Again, we use scaling arguments: consider the reference element $\widehat{K} \subset]0, 1[^2$. First of all, from Lemma 4.10, the equivalence of all norms on $\mathcal{P}_1(\mathbb{R}^2)$ and continuity of the $L^2(\widehat{K})$–projection onto $\mathcal{P}_1(\mathbb{R}^2)$, we obtain the estimate

$$\|(Id - \widehat{\mathsf{P}}_{\widehat{\omega}})\widehat{\mathsf{Q}}\widehat{u}\|_{0,\widehat{K}} \leq C\widehat{\omega}^2\|\widehat{\mathsf{Q}}\widehat{u}\|_{0,]0,1[^2} \leq C\widehat{\omega}^2\|\widehat{\mathsf{Q}}\widehat{u}\|_{0,\widehat{K}} \leq C\widehat{\omega}^2\|\widehat{u}\|_{0,\widehat{K}} \quad \forall u \in H^2(K) , \tag{4.53}$$

with a constant $C > 0$ independent of $\widehat{\omega}$. Then, by the triangle inequality, we get

$$\|(Id - \widehat{\mathsf{P}}_{\widehat{\omega}})\widehat{u}\|_{0,\widehat{K}} \leq \|(Id - \widehat{\mathsf{P}}_{\widehat{\omega}}\widehat{\mathsf{Q}})\widehat{u}\|_{0,\widehat{K}} \leq \|\widehat{u} - \widehat{\mathsf{Q}}\widehat{u}\|_{0,\widehat{K}} + \|(Id - \widehat{\mathsf{P}}_{\widehat{\omega}})\widehat{\mathsf{Q}}\widehat{u}\|_{0,\widehat{K}}$$

$$\overset{\text{proj. est.}}{\leq} C\,|\widehat{u}|_{2,\widehat{K}} + \|(Id - \widehat{\mathsf{P}}_{\widehat{\omega}})\widehat{\mathsf{Q}}\widehat{u}\|_{0,\widehat{K}} \overset{(4.53)}{\leq} C\,|\widehat{u}|_{2,\widehat{K}} + C\widehat{\omega}^2\|\widehat{u}\|_{0,\widehat{K}} .$$

Now, taking into account that transformation to the reference element changes the frequency according to $\widehat{\omega} = h_K\omega$, the result is an immediate consequence of norm transformation estimates. $\square$

PROPOSITION 4.13. *For odd $p \geq 5$ we have, with $C > 0$ independent of K and $\omega \geq 0$*

$$|(Id - \mathsf{P}_\omega)u|_{1,K} \leq Ch_K(\omega h_K + 1)(|u|_{2,K} + \omega^2\|u\|_{0,K}) \quad \forall u \in H^2(K) .$$

Proof. By the triangle inequality we have

$$|(Id - \mathsf{P}_\omega)u|_{1,K} \leq |u - \mathsf{Q}u|_{1,K} + |(Id - \mathsf{P}_\omega)\mathsf{Q}u|_{1,K} + |\mathsf{P}_\omega(\mathsf{Q}u - u)|_{1,K} . \qquad (4.54)$$

Owing to (4.52), for the first term we get

$$|u - \mathsf{Q}u|_{1,K} \leq Ch_K|u|_{2,K} , \qquad (4.55)$$

with $C > 0$ independent of K and, obviously, of ω. To tackle second term we appeal to Proposition 4.9 and use transformation to the reference triangle $\widehat{K}$

$$
\begin{aligned}
|(Id - \mathsf{P}_\omega)\mathsf{Q}u|_{1,K} &= |(Id - \widehat{\mathsf{P}}_{\widehat{\omega}})\widehat{\mathsf{Q}}\widehat{u}|_{1,\widehat{K}} \leq |(Id - \widehat{\mathsf{P}}_{\widehat{\omega}})\widehat{\mathsf{Q}}\widehat{u}|_{1,]0,1[^2} \\
&\overset{\text{Prop. 4.9}}{\leq} C(1+\widehat{\omega})\|(Id - \widehat{\mathsf{P}}_{\widehat{\omega}})\widehat{\mathsf{Q}}\widehat{u}\|_{0,]0,1[^2} \\
&\overset{\text{Lemma 4.10}}{\leq} C(1+\widehat{\omega})\widehat{\omega}^2\|\widehat{\mathsf{Q}}u\|_{0,]0,1[^2} \overset{(*)}{\leq} C(1+\widehat{\omega})\widehat{\omega}^2\|\widehat{\mathsf{Q}}u\|_{0,\widehat{K}} \\
&\leq C(1+\widehat{\omega})\widehat{\omega}^2\|u\|_{0,\widehat{K}} \leq C(1+h_K\omega)\omega^2 h_K\|u\|_{0,K} .
\end{aligned}
\qquad (4.56)
$$

again with $C > 0$ independent of K and ω. Step $(*)$ appeals to the equivalence of the L^2–norms of affine linear functions on different compact sets. The last step relies on the transformation of L^2–norm under scaling and uses $\widehat{\omega} = h_K\omega$.

Eventually, the third term allows the bounds

$$
\begin{aligned}
|\mathsf{P}_\omega(\mathsf{Q}u - u)|_{1,K} &\overset{\text{Thm. 4.8}}{\leq} C(\omega h_K + 1)h_K^{-1}\|\mathsf{P}_\omega(\mathsf{Q}u - u)\|_{0,K} \\
&\overset{\text{cont. of } \mathsf{P}_\omega}{\leq} C(\omega h_K + 1)h_K^{-1}\|\mathsf{Q}u - u\|_{0,K} \\
&\overset{\text{proj. est.}}{\leq} C(\omega h_K^2 + h_K)|u|_{2,K} .
\end{aligned}
\qquad (4.57)
$$

Also in this case the constants can be chosen independently of K and ω. Inserting (4.55)–(4.57) into (4.54) gives the assertion. $\square$

PROPOSITION 4.14. *For odd $p \geq 5$ we have, with $C > 0$ independent of K and $\omega \geq 0$,*

$$|\mathsf{P}_\omega u|_{2,K} \leq C(\omega h_K + 1)^2\big(|u|_{2,K} + \omega^2\|u\|_{0,K}\big) \quad \forall u \in H^2(K) .$$

Proof. Since the second derivatives of $\mathsf{Q}u$ vanish, the triangle inequality gives

$$|\mathsf{P}_\omega u|_{2,K} \leq |\mathsf{P}_\omega(u - \mathsf{Q}u)|_{2,K} + |(\mathsf{P}_\omega - Id)\mathsf{Q}u|_{2,K} . \qquad (4.58)$$

Since $PW_\omega^{p,0}$ is invariant w.r.t. forming partial derivatives, we have

$$
\begin{aligned}
|\mathsf{P}_\omega(u - \mathsf{Q}u)|_{2,K} &\overset{\text{Thm. 4.8}}{\leq} C_{\text{inv}}(\omega h_K + 1)h_K^{-1}|\mathsf{P}_\omega(u - \mathsf{Q}u)|_{1,K} \\
&\overset{(4.57)}{\leq} C(\omega h_K + 1)^2|u|_{2,K} ,
\end{aligned}
\qquad (4.59)
$$

with $C > 0$ independent of h_K and ω, and

$$
\begin{aligned}
|(\mathsf{P}_\omega - Id)\mathsf{Q}u|_{2,K} &\overset{\text{Prop. 4.9}}{\leq} C(\omega h_K + 1)h_K^{-1}|(\mathsf{P}_\omega - Id)\mathsf{Q}u|_{1,K} \\
&\overset{(4.56)}{\leq} C(\omega h_K + 1)h_K^{-1}(\omega^3 h_K^2 + \omega^2 h_K)\|u\|_{0,K} \\
&= C(\omega h_K + 1)(\omega^3 h_K + \omega^2)\|u\|_{0,K} ,
\end{aligned}
\qquad (4.60)
$$

again with $C > 0$ independent of h_K and ω. Inserting (4.59) and (4.60) into (4.58) gives the result. $\square$

5. Convergence analysis. Duality arguments are the linchpin of our analysis, and, inevitably, they hinge on elliptic lifting estimates for the Helmholtz operator, *cf.* [6, Sect. 5.8]. Thus, from now on, we assume that Ω is a *convex* polygon. We also recall that $\mathcal{T}_h$ is a triangular mesh with possible hanging nodes satisfying Assumption 4.6.1.

Set

$$V_h = \{v \in L^2(\Omega) \ : \ v_{|K} \in PW_\omega^{p,0}(\mathbb{R}^2) \ \forall K \in \mathcal{T}_h\} , \tag{5.1}$$

and let $V \subseteq H^2(\Omega)$ be the space containing all possible solutions u to (1.1).

In this section, we study the convergence of the method introduced in Section 3, with V_h as trial and test space. To this end, consider formulation (3.5), which is equivalent to (3.7) for our choice of V_h, with numerical fluxes given by (3.10) and (3.11).

Adding (3.5) over all elements and expanding the expressions of the numerical fluxes, with α as in (3.12) (we keep general β and δ, for the moment), we can write the primal DG method as follows: find $u_h \in V_h$ such that, for all $v_h \in V_h$,

$$a_h(u_h, v_h) - \omega^2(u_h, v_h) = (f, v_h) - \int_{\mathcal{F}_h^{\mathcal{B}}} \delta \frac{1}{i\omega} g \, \overline{\nabla_h v_h \cdot \boldsymbol{n}} \, \mathrm{d}S + \int_{\mathcal{F}_h^{\mathcal{B}}} (1-\delta) \, g \, \overline{v}_h \, \mathrm{d}S , \tag{5.2}$$

where $a_h(\cdot, \cdot)$ is the DG–bilinear form on $(V + V_h) \times (V + V_h)$ defined by

$$\begin{aligned}
a_h(u, v) =& (\nabla_h u, \nabla_h v) - \int_{\mathcal{F}_h^{\mathcal{I}}} [\![u]\!]_N \cdot \{\!\!\{\overline{\nabla_h v}\}\!\!\} \, \mathrm{d}S - \int_{\mathcal{F}_h^{\mathcal{I}}} \{\!\!\{\nabla_h u\}\!\!\} \cdot [\![\overline{v}]\!]_N \, \mathrm{d}S \\
& - \int_{\mathcal{F}_h^{\mathcal{B}}} \delta \, u \, \overline{\nabla_h v \cdot \boldsymbol{n}} \, \mathrm{d}S - \int_{\mathcal{F}_h^{\mathcal{B}}} \delta \, \nabla_h u \cdot \boldsymbol{n} \, \overline{v} \, \mathrm{d}S \\
& - \frac{1}{i\omega} \int_{\mathcal{F}_h^{\mathcal{I}}} \beta [\![\nabla_h u]\!]_N [\![\overline{\nabla_h v}]\!]_N \, \mathrm{d}S - \frac{1}{i\omega} \int_{\mathcal{F}_h^{\mathcal{B}}} \delta \, \nabla_h u \cdot \boldsymbol{n} \, \overline{\nabla_h v \cdot \boldsymbol{n}} \, \mathrm{d}S \\
& + i \int_{\mathcal{F}_h^{\mathcal{I}}} \frac{\mathsf{a}}{\mathsf{h}} [\![u]\!]_N \cdot [\![\overline{v}]\!]_N \, \mathrm{d}S + i\omega \int_{\mathcal{F}_h^{\mathcal{B}}} (1-\delta) \, u \, \overline{v} \, \mathrm{d}S .
\end{aligned} \tag{5.3}$$

PROPOSITION 5.1. *If $\beta > 0$, $0 < \delta < 1$, and a is uniformly positive, the discrete variational problem (5.2) possesses a unique solution for any $f \in L^2(\Omega)$ and $g \in L^2(\partial\Omega)$.*

Proof. Note that $\mathrm{Im}\,(a_h(v_h, v_h)) > 0$ for all $v_h \in V_h$. □

The DG method (5.2) is consistent by construction, and thus, if u is the analytical solution of (1.1),

$$a_h(u - u_h, v_h) = \omega^2(u - u_h, v_h) \qquad \forall v_h \in V_h. \tag{5.4}$$

Taking the cue from the definition of $a_h(\cdot, \cdot)$, we define the following mesh-dependent seminorm and norms on $V + V_h$:

$$\begin{aligned}
|v|_{DG}^2 :=& \|\nabla_h v\|_{0,\Omega}^2 + \omega^{-1} \|\beta^{1/2} [\![\nabla_h v]\!]_N\|_{0,\mathcal{F}_h^{\mathcal{I}}}^2 + \|\mathsf{a}^{1/2} \mathsf{h}^{-1/2} [\![v]\!]_N\|_{0,\mathcal{F}_h^{\mathcal{I}}}^2 \\
& + \omega^{-1} \|\delta^{1/2} \nabla_h v \cdot \boldsymbol{n}\|_{0,\mathcal{F}_h^{\mathcal{B}}}^2 + \omega \|(1-\delta)^{1/2} v\|_{0,\mathcal{F}_h^{\mathcal{B}}}^2,
\end{aligned}$$

$$\|v\|_{DG}^2 := |v|_{DG}^2 + \omega^2 \|v\|_{0,\Omega}^2,$$

$$\|v\|_{DG^+}^2 := \|v\|_{DG}^2 + \omega \|\beta^{-1/2} \{\!\!\{v\}\!\!\}\|_{0,\mathcal{F}_h^{\mathcal{I}}}^2 + \|\mathsf{a}^{-1/2} \mathsf{h}^{1/2} \{\!\!\{\nabla_h v\}\!\!\}\|_{0,\mathcal{F}_h^{\mathcal{I}}}^2 + \omega \|\delta^{-1/2} v\|_{0,\mathcal{F}_h^{\mathcal{B}}}^2.$$

We prove that the auxiliary DG–bilinear form, which is related to the positive operator $-\Delta + \omega^2$,

$$b_h(u, v) := a_h(u, v) + \omega^2(u, v)$$

is coercive in the DG–norm. To this end, we apply the inverse inequality for plane waves asserted in Theorem 4.7.

PROPOSITION 5.2. *With the particular choice of $\alpha = \mathsf{a}/\omega\mathsf{h}$ (see (3.12)), with $\mathsf{a} \geq \mathsf{a}_{\min} > C^2_{\mathrm{tinv}}$, and $0 < \delta < 1/2$ in the numerical fluxes (3.10) and (3.11), there exists a constant $C_{\mathrm{coer}} > 0$ only depending on α_0 from Assumption 4.6.1, in particular, independent of ω and of the mesh, such that*

$$|b_h(v,v)| \geq C_{\mathrm{coer}}\|v\|^2_{DG} \qquad \forall v \in V_h.$$

Proof. By definition, we have

$$\begin{aligned}
b_h(v,v) =&\|\nabla_h u\|^2_{0,\Omega} - 2\,\mathrm{Re}\,\left(\int_{\mathcal{F}^{\mathcal{I}}_h} [\![v]\!]_N \cdot \{\!\!\{\overline{\nabla_h v}\}\!\!\}\,\mathrm{d}S\right) - 2\,\mathrm{Re}\,\left(\int_{\mathcal{F}^{\mathcal{B}}_h} \delta\,v\,\overline{\nabla_h v \cdot \boldsymbol{n}}\,\mathrm{d}S\right)\\
&+ i\omega^{-1}\|\beta^{1/2}[\![\nabla_h v]\!]_N\|^2_{0,\mathcal{F}^{\mathcal{I}}_h} + i\omega^{-1}\|\delta^{1/2}\nabla_h v \cdot \boldsymbol{n}\|^2_{0,\mathcal{F}^{\mathcal{B}}_h}\\
&+ i\,\|\mathsf{a}^{1/2}\mathsf{h}^{-1/2}[\![v]\!]_N\|^2_{0,\mathcal{F}^{\mathcal{I}}_h} + i\omega\,\|(1-\delta)^{1/2}v\|^2_{0,\mathcal{F}^{\mathcal{B}}_h} + \omega^2\|v\|^2_{0,\Omega}.
\end{aligned}$$
(5.5)

From the weighted Cauchy-Schwarz inequality and the Young inequality, we obtain, for $s > 0$ at disposal,

$$\begin{aligned}
\left|2\,\mathrm{Re}\,\int_{\mathcal{F}^{\mathcal{I}}_h} [\![v]\!]_N \cdot \{\!\!\{\overline{\nabla_h v}\}\!\!\}\,\mathrm{d}S\right| \leq& s\,\|\mathsf{h}^{-1/2}[\![v]\!]_N\|^2_{0,\mathcal{F}^{\mathcal{I}}_h} + \frac{1}{s}\,\|\mathsf{h}^{1/2}\{\!\!\{\nabla_h v\}\!\!\}\|^2_{0,\mathcal{F}^{\mathcal{I}}_h}\\
\leq& \frac{s}{\mathsf{a}_{\min}}\,\|\mathsf{a}^{1/2}\mathsf{h}^{-1/2}[\![v]\!]_N\|^2_{0,\mathcal{F}^{\mathcal{I}}_h} + \frac{C^2_{\mathrm{tinv}}}{s}\,\|\nabla_h v\|^2_{0,\Omega}\,,
\end{aligned}$$
(5.6)

where in the last step we have used the inverse inequality of Theorem 4.7; similarly, for $t > 0$ at disposal, we have

$$\left|2\,\mathrm{Re}\,\int_{\mathcal{F}^{\mathcal{B}}_h} \delta\,v\,\overline{\nabla_h v}\,\mathrm{d}S\right| \leq t\,\omega\,\frac{\delta}{1-\delta}\,\|(1-\delta)^{1/2}v\|^2_{0,\mathcal{F}^{\mathcal{B}}_h} + \frac{1}{t\,\omega}\,\|\delta^{1/2}\nabla_h v\|^2_{0,\mathcal{F}^{\mathcal{B}}_h}. \quad (5.7)$$

Since $0 < \delta < 1/2$ and $\mathsf{a}_{\min} > C^2_{\mathrm{tinv}}$, if s and t are such that $s > C^2_{\mathrm{inv}}$ and $t > 1$, inserting (5.6) and (5.5) into (5.5) gives

$$\begin{aligned}
|b_h(v,v)| \geq& \frac{1}{\sqrt{2}}\,[|\mathrm{Re}\,(b_h(v,v))| + |\mathrm{Im}\,(b_h(v,v))|]\\
\geq& \frac{1}{\sqrt{2}}\left[\left(1 - \frac{C^2_{\mathrm{tinv}}}{s}\right)\|\nabla_h v\|^2_{0,\Omega} + \left(1 - \frac{s}{\mathsf{a}_{\min}}\right)\|\mathsf{a}^{1/2}\mathsf{h}^{-1/2}[\![v]\!]_N\|^2_{0,\mathcal{F}^{\mathcal{I}}_h}\right.\\
&+ \omega\left(1 - t\frac{\delta}{1-\delta}\right)\|(1-\delta)^{1/2}v\|^2_{0,\mathcal{F}^{\mathcal{B}}_h} + \omega^{-1}\left(1 - \frac{1}{t}\right)\|\delta^{1/2}\nabla_h v \cdot \boldsymbol{n}\|^2_{0,\mathcal{F}^{\mathcal{B}}_h}\\
&\left.+ \omega^{-1}\|\beta^{1/2}[\![\nabla_h v]\!]_N\|^2_{0,\mathcal{F}^{\mathcal{I}}_h} + \omega^2\|v\|^2_{0,\Omega}\right]\\
\geq& C\|v\|^2_{DG},
\end{aligned}$$

with $C > 0$ independent of the mesh and ω. $\square$

REMARK 5.3. *For the original formulation of Cessenat and Despres [9] where $\mathsf{a} = \omega\mathsf{h}/2$, the coercivity stated in Proposition 5.2 remains elusive. Still, Proposition 5.1*

confirms existence and uniqueness of discrete solutions, which Cessenat and Despres proved in a completely different fashion.

We develop the theoretical analysis of the method (5.2) by using Schatz' duality argument [23]. We start by stating the following abstract estimate.

PROPOSITION 5.4. *If u is the analytical solution to (1.1) and $u_h \in V_h$ defined as in (5.1) is the discrete solution to (3.7) with numerical fluxes (3.10) and (3.11) (α and δ as in Proposition 5.2), then*

$$\|u - u_h\|_{DG} \le C_{\mathrm{abs}} \left(\inf_{v_h \in V_h} \|u - v_h\|_{DG^+} + \sup_{0 \ne w_h \in V_h} \frac{\omega \, |(u - u_h, w_h)|}{\|w_h\|_{0,\Omega}} \right) , \qquad (5.8)$$

where $C_{\mathrm{abs}} > 0$ is a constant independent of the mesh and ω.

Proof. By the triangle inequality, for all $v_h \in V_h$, it holds

$$\|u - u_h\|_{DG} \le \|u - v_h\|_{DG} + \|v_h - u_h\|_{DG}. \qquad (5.9)$$

From the coercivity in Proposition 5.2, the definition of $b_h(\cdot, \cdot)$ and (5.4), we get

$$
\begin{aligned}
\|v_h - u_h\|_{DG}^2 \le & \frac{1}{C_{\mathrm{coer}}} |b_h(v_h - u_h, v_h - u_h)| \\
\le & \frac{1}{C_{\mathrm{coer}}} |b_h(v_h - u, v_h - u_h)| + \frac{1}{C_{\mathrm{coer}}} |b_h(u - u_h, v_h - u_h)| \qquad (5.10) \\
= & \frac{1}{C_{\mathrm{coer}}} |b_h(v_h - u, v_h - u_h)| + \frac{1}{C_{\mathrm{coer}}} 2\omega^2 |(u - u_h, v_h - u_h)|.
\end{aligned}
$$

We estimate the first term on the right-hand side of (5.10). Setting $w_h := v_h - u_h$, integrating by parts and taking into account that $-\Delta_h w_h = \omega^2 w_h$, we can write

$$
\begin{aligned}
(\nabla_h(v_h - u), \nabla_h w_h) = & \sum_{K \in \mathcal{T}_h} \left[-\int_K (v_h - u)\overline{\Delta w_h} \, dV + \int_{\partial K} (v_h - u)\overline{\nabla_h w_h \cdot \boldsymbol{n}} \, dS \right] \\
= & \omega^2 (v_h - u, w_h) + \int_{\mathcal{F}_h^{\mathcal{I}}} [\![v_h - u]\!]_N \cdot \{\!\{ \overline{\nabla_h w_h} \}\!\} \, dS \\
& + \int_{\mathcal{F}_h^{\mathcal{I}}} \{\!\{ v_h - u \}\!\} [\![\overline{\nabla_h w_h}]\!]_N \, dS + \int_{\mathcal{F}_h^{\mathcal{B}}} (v_h - u)\overline{\nabla_h w_h \cdot \boldsymbol{n}} \, dS ,
\end{aligned}
$$

where we have used the usual "DG magic formula" to write the sum over all elements of integrals over element boundaries as in terms of integrals over the mesh skeleton.

Thus, using the definition of $b_h(\cdot,\cdot)$, we have

$$
\begin{aligned}
b_h(v_h - u, w_h) = {} & 2\,\omega^2(v_h - u, w_h) + \int_{\mathcal{F}_h^{\mathcal{I}}} \{\!\!\{ v_h - u \}\!\!\} \llbracket \overline{\nabla_h w_h} \rrbracket_N \, \mathrm{d}S \\
& + \int_{\mathcal{F}_h^{\mathcal{B}}} (v_h - u)\overline{\nabla_h w_h \cdot \boldsymbol{n}} \, \mathrm{d}S - \int_{\mathcal{F}_h^{\mathcal{I}}} \{\!\!\{ \nabla_h(v_h - u) \}\!\!\} \cdot \llbracket w_h \rrbracket_N \, \mathrm{d}S \\
& - \int_{\mathcal{F}_h^{\mathcal{B}}} \delta(v_h - u)\overline{\nabla_h w_h \cdot \boldsymbol{n}} \, \mathrm{d}S - \int_{\mathcal{F}_h^{\mathcal{B}}} \delta\nabla_h(v_h - u) \cdot \boldsymbol{n}\, \overline{w_h} \, \mathrm{d}S \\
& + \frac{i}{\omega} \int_{\mathcal{F}_h^{\mathcal{I}}} \beta \llbracket \nabla_h(v_h - u) \rrbracket_N \llbracket \overline{\nabla_h w_h} \rrbracket_N \, \mathrm{d}S \\
& + \frac{i}{\omega} \int_{\mathcal{F}_h^{\mathcal{B}}} \delta\nabla_h(v_h - u) \cdot \boldsymbol{n}\, \overline{\nabla_h w_h \cdot \boldsymbol{n}} \, \mathrm{d}S \\
& + i \int_{\mathcal{F}_h^{\mathcal{I}}} \frac{\mathsf{a}}{\mathsf{h}} \llbracket v_h - u \rrbracket_N \llbracket \overline{w_h} \rrbracket \, \mathrm{d}S + i\omega \int_{\mathcal{F}_h^{\mathcal{B}}} (1 - \delta)(v_h - u)\overline{w_h} \, \mathrm{d}S \, .
\end{aligned}
$$

Therefore, by repeatedly applying the Cauchy-Schwarz inequality with appropriate weights, we obtain

$$
|b_h(v_h - u, w_h)| \le C\, \|v_h - u\|_{DG+} \|w_h\|_{DG} \, ,
$$

with $C > 0$ only depending on α_0. Inserting this into (5.10) and taking into account (5.9) gives the result. $\square$

We have to bound the term $\displaystyle\sup_{0 \ne w_h \in V_h} \frac{\omega\,|(u - u_h, w_h)|}{\|w_h\|_{0,\Omega}}$ in the estimate of Proposition 5.4 by using a duality argument. To this end, we have to adopt the special choice (3.12) of all the numerical flux parameters, with the additional constraints $\mathsf{a}_{\min} > C_{\mathrm{tinv}}^2$ and $0 < \delta < 1/2$. Then the DG seminorm and norms can be explicitly written as follows:

$$
\begin{aligned}
|v|_{DG}^2 = {} & \|\nabla_h v\|_{0,\Omega}^2 + \|\mathsf{b}^{1/2}\mathsf{h}^{1/2}\llbracket \nabla_h v \rrbracket_N\|_{0,\mathcal{F}_h^{\mathcal{I}}}^2 + \|\mathsf{a}^{1/2}\mathsf{h}^{-1/2}\llbracket v \rrbracket_N\|_{0,\mathcal{F}_h^{\mathcal{I}}}^2 \\
& + \|\mathsf{d}^{1/2}\mathsf{h}^{1/2}\nabla_h v \cdot \boldsymbol{n}\|_{0,\mathcal{F}_h^{\mathcal{B}}}^2 + \|(\omega - \mathsf{d}\omega^2\mathsf{h})^{1/2}v\|_{0,\mathcal{F}_h^{\mathcal{B}}}^2, \\
\|v\|_{DG}^2 = {} & |v|_{DG}^2 + \omega^2\|v\|_{0,\Omega}^2, \\
\|v\|_{DG+}^2 = {} & \|v\|_{DG}^2 + \|\mathsf{b}^{-1/2}\mathsf{h}^{-1/2}\{\!\!\{ v \}\!\!\}\|_{0,\mathcal{F}_h^{\mathcal{I}}}^2 + \|\mathsf{a}^{-1/2}\mathsf{h}^{1/2}\{\!\!\{ \nabla_h v \}\!\!\}\|_{0,\mathcal{F}_h^{\mathcal{I}}}^2 \\
& + \|\omega^{1/2}\mathsf{d}^{-1/2}\mathsf{h}^{-1/2}v\|_{0,\mathcal{F}_h^{\mathcal{B}}}^2.
\end{aligned}
$$

We will make use of the following regularity theorem proved in [20]. Its original statement makes use of the following weighted norm on $H^1(\Omega)$:

$$
\|v\|_{1,\omega,\Omega}^2 = |v|_{1,\Omega}^2 + \omega^2\|v\|_{0,\Omega}^2 \, . \tag{5.11}
$$

THEOREM 5.5. *[20, Proposition 8.1.4] Let Ω be a bounded convex domain (or smooth and star-shaped). Consider the adjoint problem to (1.1) with right-hand side $w \in L^2(\Omega)$:*

$$
\begin{aligned}
-\Delta\varphi - \omega^2\varphi &= w && \text{in } \Omega, \\
-\nabla\varphi \cdot \boldsymbol{n} + i\omega\,\varphi &= 0 && \text{on } \partial\Omega.
\end{aligned} \tag{5.12}
$$

Then, the solution φ belongs to $H^2(\Omega)$, and

$$\|\varphi\|_{1,\omega,\Omega} \leq C_1(\Omega)\|w\|_{0,\Omega} \,,$$
$$|\varphi|_{2,\Omega} \leq C_2(\Omega)\,(1+\omega)\,\|w\|_{0,\Omega} \,, \tag{5.13}$$

with $C_1(\Omega), C_2(\Omega) > 0$.

The next lemma provides L^2–projection error estimates for traces onto the skeleton of $\mathcal{T}_h$. In light of the definitions of the DG and DG^+ seminorms and norms, these are essential. We keep the notation P_ω for the $L^2(\Omega)$–orthogonal projection onto V_h, see (5.1).

LEMMA 5.6. *Let the assumptions of Theorem 5.5 hold true. Then there is $c_0 > 0$ such that, provided that $\omega^2 h \leq c_0$, the solution φ of* (5.12) *allows the estimates*

$$\left\{ \begin{array}{c} \|\mathsf{h}^{-1/2}(\varphi - \mathsf{P}_\omega\varphi)\|_{0,\mathcal{F}_h}^2 \\ \|\mathsf{h}^{1/2}\nabla_h(\varphi - \mathsf{P}_\omega\varphi)\|_{0,\mathcal{F}_h}^2 \end{array} \right\} \leq Ch(h+c_0)\|w\|_{0,\Omega}^2 \,, \tag{5.14}$$

with $C > 0$ depending only on the bound for the minimal angle of elements and the domain Ω.

Proof. We start with local considerations: we recall the multiplicative trace inequality for $K \in \mathcal{T}_h$, see [6, Theorem 1.6.6],

$$\|u\|_{0,\partial K}^2 \leq C\|u\|_{0,K}\big(h_K^{-1}\|u\|_{0,K} + |u|_{1,K}\big) \quad \forall u \in H^1(K) \,. \tag{5.15}$$

Here and in the rest of the proof constants $C > 0$ may only depend on the bound for the minimal angle of K, *cf.* Assumption 4.6.1, and the domain Ω. Hence,

$$h_K^{-1}\|\varphi - \mathsf{P}_\omega\varphi\|_{0,\partial K}^2 \leq Ch_K^{-1}\|\varphi - \mathsf{P}_\omega\varphi\|_{0,K}\big(h_K^{-1}\|\varphi - \mathsf{P}_\omega\varphi\|_{0,K} + |\varphi - \mathsf{P}_\omega\varphi|_{1,K}\big)$$
$$\leq Ch_K^2(\omega h_K + 1)\big(|\varphi|_{2,K} + \omega^2\|\varphi\|_{0,K}\big)^2 \,,$$

where the last estimate invokes Propositions 4.12 and 4.13. Similarly,

$$h_K\|\nabla_h(\varphi - \mathsf{P}_\omega\varphi)\|_{0,\partial K}^2 \leq Ch_K|\varphi - \mathsf{P}_\omega\varphi|_{1,K}\big(h_K^{-1}|\varphi - \mathsf{P}_\omega\varphi|_{1,K} + |\varphi - \mathsf{P}_\omega\varphi|_{2,K}\big)$$
$$\leq Ch_K^2(\omega h_K + 1)^3\big(|\varphi|_{2,K} + \omega^2\|\varphi\|_{0,K}\big)^2 \,.$$

The last step relies on Propositions 4.13 and 4.14. Next, we sum over all elements, apply the Cauchy-Schwarz inequality, and use the estimates (5.13) of Theorem 5.5:

$$\|\mathsf{h}^{-1/2}(\varphi - \mathsf{P}_\omega\varphi)\|_{0,\mathcal{F}_h}^2 \leq Ch^2(\omega h + 1)(1+\omega)^2\|w\|_{0,\Omega}^2 \leq Ch(h+c_0)\|w\|_{0,\Omega}^2 \,,$$
$$\|\mathsf{h}^{1/2}\nabla_h(\varphi - \mathsf{P}_\omega\varphi)\|_{0,\mathcal{F}_h}^2 \leq Ch^2(\omega h + 1)^3(1+\omega)^2\|w\|_{0,\Omega}^2 \leq Ch(h+c_0)\|w\|_{0,\Omega}^2 \,.$$

Here, the assumption $\omega^2 h \leq c_0$ comes into play, which also guarantees that ωh is bounded. $\square$

COROLLARY 5.7. *Let the assumptions of Theorem 5.5 hold true. Then there is $c_0 > 0$ such that, provided that $\omega^2 h \leq c_0$, the solution φ of* (5.12) *allows the estimates*

$$\omega^2\|\varphi - \mathsf{P}_\omega\varphi\|_{0,\Omega}^2 \leq Ch^2 c_0(h+c_0)\|w\|_{0,\Omega}^2 \,, \tag{5.16}$$
$$\|\varphi - \mathsf{P}_\omega\varphi\|_{DG^+}^2 \leq Ch(h+c_0)\|w\|_{0,\Omega}^2 \,, \tag{5.17}$$
$$\omega^2\|\varphi - \mathsf{P}_\omega\varphi\|_{DG^+}^2 \leq Cc_0(h+c_0)\|w\|_{0,\Omega}^2 \,, \tag{5.18}$$

with $C > 0$ *depending only on the bound for the minimal angle of elements, the geometry of Ω, and the constants* a*,* b *and* d *in the definition of the numerical fluxes.*

Proof. The first two bounds follow from Propositions 4.12, 4.13 and Lemma 5.6; the third bound is a simple application of the assumption $\omega^2 h \leq c_0$ to the second bound. □

PROPOSITION 5.8. *Let the assumptions of Theorem 5.5 hold true. Then there is $c_0 > 0$, such that, provided that $\omega^2 h \leq c_0$, the following estimate holds true:*

$$\sup_{0 \neq w_h \in V_h} \frac{\omega |(u - u_h, w_h)|}{\|w_h\|_{0,\Omega}} \leq C_{\mathrm{dual}} \left[c_0 (h + c_0) \right]^{1/2} \left(\|u - u_h\|_{DG} + h \|f - \mathsf{P}_\omega f\|_{0,\Omega} \right),$$

with a constant $C_{\mathrm{dual}} > 0$ independent of the mesh and ω.

Proof. Consider the adjoint problem (5.12) with right-hand side $w_h \in V_h \subset L^2(\Omega)$. Then, from Theorem 5.5, we have that $\varphi \in H^2(\Omega)$, $\|\varphi\|_{1,\omega,\Omega} \leq C_1(\Omega) \|w_h\|_{0,\Omega}$ and $|\varphi|_{2,\Omega} \leq C_2(\Omega) (1 + \omega) \|w_h\|_{0,\Omega}$, with $C_1(\Omega), C_2(\Omega) > 0$. Moreover, this solution φ satisfies

$$a_h(\psi, \varphi) - \omega^2(\psi, \varphi) = (\psi, w_h) \qquad \forall \psi \in V. \tag{5.19}$$

The adjoint consistency of the DG method (see Section 3) implies that

$$a_h(\psi_h, \varphi) - \omega^2(\psi_h, \varphi) = (\psi_h, w_h) \qquad \forall \psi_h \in V_h. \tag{5.20}$$

Taking into account adjoint consistency and consistency, i.e., (5.20) and (5.4), respectively, we have, for all $\psi_h \in V_h$,

$$(u - u_h, w_h) = (u, w_h) - (u_h, w_h) \overset{(5.19)}{=} a_h(u, \varphi) - \omega^2(u, \varphi) - (u_h, w_h)$$

$$\overset{(5.20)}{=} a_h(u, \varphi) - \omega^2(u, \varphi) - a_h(u_h, \varphi) + \omega^2(u_h, \varphi)$$

$$= a_h(u - u_h, \varphi) - \omega^2(u - u_h, \varphi)$$

$$\overset{(5.4)}{=} a_h(u - u_h, \varphi - \psi_h) - \omega^2(u - u_h, \varphi - \psi_h).$$

Using the definition of $a_h(\cdot, \cdot)$, integrating by parts the gradient term and taking into account that $-\Delta u - \omega^2 u = f$ and $-\Delta_h u_h - \omega^2 u_h = 0$, we get

$$(u - u_h, w_h) = (f, \varphi - \psi_h) + \int_{\mathcal{F}_h^{\mathcal{I}}} [\![\nabla_h(u - u_h)]\!]_N \{\!\{\overline{\varphi - \psi_h}\}\!\} \, dS$$

$$+ \int_{\mathcal{F}_h^{\mathcal{B}}} \nabla_h(u - u_h) \cdot \boldsymbol{n} \, (\overline{\varphi - \psi_h}) \, dS - \int_{\mathcal{F}_h^{\mathcal{I}}} [\![u - u_h]\!]_N \cdot \{\!\{\overline{\nabla_h(\varphi - \psi_h)}\}\!\} \, dS$$

$$- \int_{\mathcal{F}_h^{\mathcal{B}}} \mathsf{d}\omega\mathsf{h} \, (u - u_h) \, \overline{\nabla_h(\varphi - \psi_h) \cdot \boldsymbol{n}} \, dS - \int_{\mathcal{F}_h^{\mathcal{B}}} \mathsf{d}\omega\mathsf{h} \, \nabla_h(u - u_h) \cdot \boldsymbol{n} \, (\overline{\varphi - \psi_h}) \, dS$$

$$+ i \int_{\mathcal{F}_h^{\mathcal{I}}} \mathsf{b}\mathsf{h} \, [\![\nabla_h(u - u_h)]\!]_N \, \overline{[\![\nabla_h(\varphi - \psi_h)]\!]_N} \, dS$$

$$+ i \int_{\mathcal{F}_h^{\mathcal{B}}} \mathsf{d}\mathsf{h} \, \nabla_h(u - u_h) \cdot \boldsymbol{n} \, \overline{\nabla_h(\varphi - \psi_h) \cdot \boldsymbol{n}} \, dS$$

$$+ i \int_{\mathcal{F}_h^{\mathcal{I}}} \frac{\mathsf{a}}{\mathsf{h}} \, [\![u - u_h]\!]_N \cdot \overline{[\![\varphi - \psi_h]\!]_N} \, dS + i \int_{\mathcal{F}_h^{\mathcal{B}}} (\omega - \mathsf{d}\omega^2\mathsf{h}) \, (u - u_h) \, (\overline{\varphi - \psi_h}) \, dS \, .$$

and thus, for all $\psi_h \in V_h$, we obtain

$$\omega |(u - u_h, w_h)| \leq C \, \|u - u_h\|_{DG} \, \omega \|\varphi - \psi_h\|_{DG^+} + \omega |(f, \varphi - \psi_h)| \, , \tag{5.21}$$

with C independent of the mesh, ω, and the flux parameters.

Actually, the estimate (5.21) holds true with $\|\varphi - \psi_h\|_{DG+}$ replaced by the interelement and boundary part of $\|\varphi - \psi_h\|_{DG+}$ only (no volume terms).

We choose $\psi_h = \mathsf{P}_\omega \varphi$, i.e., the $L^2(\Omega)$–projection of φ onto V_h. Since

$$\omega|(f, \varphi - \psi_h)| = \omega|(f - \mathsf{P}_\omega f, \varphi - \psi_h)| \leq \|f - \mathsf{P}_\omega f\|_{0,\Omega} \, \omega \|\varphi - \psi_h\|_{0,\Omega} \,,$$

the result follows from Corollary 5.7. $\square$

The following estimate of the DG–norm of the error is a direct consequence of Proposition 5.4, Proposition 5.8 and of the following best approximation estimate.

LEMMA 5.9. *For any $w \in H^2(\Omega)$, we have*

$$\inf_{v_h \in V_h} \|w - v_h\|_{DG+} \leq Ch(\omega h + 1)^{3/2} \left(|w|_{2,\Omega} + \omega^2 \|w\|_{0,\Omega} \right) \,,$$

with a constant $C > 0$ independent of the mesh and ω.

Proof. We bound $\inf_{v_h \in V_h} \|w - v_h\|_{DG+}$ by $\|w - \mathsf{P}_\omega w\|_{DG+}$ and proceed as in Lemma 5.6 and Corollary 5.7. $\square$

THEOREM 5.10. *Let the assumptions of Theorem 5.5 hold true and impose $\mathsf{a}_{\min} > C_{\mathrm{tinv}}^2$ and $0 < \delta < \frac{1}{2}$ on the parameters of the plane wave discontinuous Galerkin method (5.2). Then there is $c_0 > 0$ such that, provided that*

$$\omega^2 h \leq c_0 \,, \tag{5.22}$$

the following a priori error estimate holds true:

$$\|u - u_h\|_{DG} \leq Ch \left(|u|_{2,\Omega} + \omega^2 \|u\|_{0,\Omega} + [c_0(h + c_0)]^{1/2} \|f - \mathsf{P}_\omega f\|_{0,\Omega} \right) \,,$$

with a constant $C > 0$ independent of the mesh and wave number ω.

Proof. From Propositions 5.4 and 5.8, provided that $C_{\mathrm{abs}} C_{\mathrm{dual}}[c_0(h + c_0)]^{1/2} < 1$, we have

$$\|u - u_h\|_{DG} \leq C \left(\inf_{v_h \in V_h} \|u - v_h\|_{DG+} + h[c_0(h + c_0)]^{1/2} \|f - \mathsf{P}_\omega f\|_{0,\Omega} \right) \,,$$

with a constant $C > 0$ independent of the mesh and ω. The result now follows from the regularity of u, Lemma 5.9 and the assumption $\omega^2 h \leq c_0$. $\square$

REMARK 5.11. *The threshold condition (5.22) requires a minimum resolution of the trial space before asymptotic convergence sets in. This reflects vulnerability to the* pollution effect *discussed in the Introduction.*

REMARK 5.12. *The mere first-order convergence asserted in Thm. 5.10 may be disappointing, but in the presence of a non-vanishing source term f no better rate can be expected, because plane waves only possess the approximating power of 1st-degree polynomials for generic functions, see Section 4.2.*

Only solution of the homogeneous Helmholtz equation, that is, the case $f = 0$, allows better approximation estimates when using more plane wave directions. More precisely, if u is sufficiently smooth and $p = 2m + 1$, we can expect $\|u - u_h\|_{DG} = O(h^m)$. The underlying approximation results are given in [20, Prop. 8.4.14]. In this paper we will not elaborate this further in the DG setting.

We conclude this section by proving a priori L^2–norm error estimates. We have the following result:

THEOREM 5.13. *Let the assumptions of Theorem 5.5 hold true. Then there is* $c_0 > 0$, *such that, provided that* $\omega^2 h \leq c_0$, *we have*

$$\|u - u_h\|_{0,\Omega} \leq C[h^3(h + c_0)]^{1/2} \left(|u|_{2,\Omega} + \omega^2 \|u\|_{0,\Omega} + [c_0(h + c_0)]^{1/2} \|f - \mathsf{P}_\omega f\|_{0,\Omega} \right),$$

with a constant $C > 0$ *independent of the mesh and wave number* ω.

Proof. Let φ be the solution to the adjoint problem (5.12) with right-hand side $w \in L^2(\Omega)$. By proceeding like in the proof of Proposition 5.8, by definition of the dual problem, consistency and adjoint consistency, we have

$$(u - u_h, w) = a_h(u - u_h, \varphi - \mathsf{P}_\omega \varphi) - \omega^2(u - u_h, \varphi - \mathsf{P}_\omega \varphi),$$

or, equivalently,

$$
\begin{aligned}
(u - u_h, w) = {} & a_h(u - v_h, \varphi - \mathsf{P}_\omega \varphi) - \omega^2(u - v_h, \varphi - \mathsf{P}_\omega \varphi) \\
& + a_h(v_h - u_h, \varphi - \mathsf{P}_\omega \varphi) - \omega^2(v_h - u_h, \varphi - \mathsf{P}_\omega \varphi)
\end{aligned}
\tag{5.23}
$$

for all $v_h \in V_h$. By repeatedly applying the Cauchy-Schwarz inequality with appropriate weights, we obtain

$$|a_h(u - v_h, \varphi - \mathsf{P}_\omega \varphi) - \omega^2(u - v_h, \varphi - \mathsf{P}_\omega \varphi)| \leq \|u - v_h\|_{DG^+} \|\varphi - \mathsf{P}_\omega \varphi\|_{DG^+},$$

whereas, since $v_h - u_h \in V_h$, proceeding as in the proof of Proposition 5.4, we get

$$|a_h(v_h - u_h, \varphi - \mathsf{P}_\omega \varphi) - \omega^2(v_h - u_h, \varphi - \mathsf{P}_\omega \varphi)| \leq \|v_h - u_h\|_{DG} \|\varphi - \mathsf{P}_\omega \varphi\|_{DG^+}.$$

By applying these estimates to the right-hand side of (5.23), we obtain

$$
\begin{aligned}
|(u - u_h, w)| & \leq (\|u - v_h\|_{DG^+} + \|v_h - u_h\|_{DG}) \|\varphi - \mathsf{P}_\omega \varphi\|_{DG^+} \\
& \leq (2\|u - v_h\|_{DG^+} + \|u - u_h\|_{DG}) \|\varphi - \mathsf{P}_\omega \varphi\|_{DG^+}
\end{aligned}
$$

for all $v_h \in V_h$. From the definition of the L^2–norm we have

$$\|u - u_h\|_{0,\Omega} \leq \left(2 \inf_{v_h \in V_h} \|u - v_h\|_{DG^+} + \|u - u_h\|_{DG} \right) \sup_{0 \neq w \in L^2(\Omega)} \frac{\|\varphi - \mathsf{P}_\omega \varphi\|_{DG^+}}{\|w\|_{0,\Omega}}.$$

The result follows from Lemma 5.9, Theorem 5.10 and Corollary 5.7. $\square$

REMARK 5.14. *In [7], an priori* L^2–*norm error estimate of the form*

$$\|u - u_h\|_{0,\Omega} \leq C h^{-1/2} \inf_{v_h \in X_h} \|u - v_h\|_X \tag{5.24}$$

for h-version of the UWVF is directly established. It is valid for $f = 0$ *and relies on an error estimate in a mesh-dependent norm proved in [9]. Here,* $\|\cdot\|_X$ *is a scaled* L^2-*norm on the skeleton of the mesh and* X_h *a plane wave type space. In contrast to our results, this estimate holds for all wave numbers, but the dependence of* C *on* ω *is not made explicit.*

For sufficiently smooth analytical solutions (5.24) yields $O(h^{m-1})$-*convergence when using* $p = 2m + 1$ *equispaced plane wave directions. The authors point out that numerical tests show that this under-estimates the actual convergence rates and conjecture that this gap might be filled by using duality arguments. It might be of interest to investigate whether our approach could actually be useful in this direction (see Remark 5.12).*

6. Duality estimate in one space dimension. The case $d = 1$ is very particular in that there are only two linearly independent plane wave solutions for the homogeneous Helmholtz equation. Thus, the plane wave space is

$$PW_\omega(\mathbb{R}) = \langle \exp(i\omega x), \exp(-i\omega x) \rangle = \langle \cos(\omega x), \sin(\omega x) \rangle .$$

(6.1)

In one dimension on $\Omega =]-1, 1[$ the adjoint problem (5.12) boils down to the two-point boundary value problem

$$-\varphi'' - \omega^2 \varphi = w_h \quad \text{in }]-1, 1[,$$

(6.2)

$$\pm \varphi'(\pm 1) - i\omega \varphi(\pm 1) = 0 .$$

(6.3)

We assume that $\Omega =]-1, 1[$ is equipped with nodes $-1 = x_0 < x_1 < \cdots < x_M = 1$, $M \in \mathbb{N}$, and a mesh $\mathcal{T}_h := \{]x_{j-1}, x_j[\}_{j=1}^M$, with midpoints $m_j := \frac{1}{2}(x_{j-1} + x_j)$. Thus, the discrete trial and test space (5.1) becomes

$$V_h := \{v \in L^2(]-1, 1[) :\ v(x) = \rho_j \cos(\omega(x - m_j)) + \kappa_j \sin(\omega(x - m_j)), \quad (6.4)$$
$$x_{j-1} < x < x_j, \ \rho_j, \kappa_j \in \mathbb{C}, \ j = 1, \ldots, M\} .$$

Hence, we may write $w_h \in V_h$ as

$$w_h = \sum_{j=1}^M \chi_{]x_{j-1}, x_j[} w_j , \quad w_j(x) = \rho_j \cos(\omega(x - m_j)) + \kappa_j \sin(\omega(x - m_j)) \in PW_\omega(\mathbb{R}) .$$

(6.5)

The 2-point boundary value problem (6.2) with right hand side $\chi_{]x_{j-1}, x_j[} w_j$ has a solution of the form

$$\varphi_j(x) = \begin{cases} A^- \cos(\omega x) + B^- \sin(\omega x), \ -1 < x < x_{j-1} \\ \rho_j s_j(x) + \kappa_j c_j(x) + A \cos(\omega(x - m_j)) + B \sin(\omega(x - m_j)), \ x_{j-1} < x < x_j \\ A^+ \cos(\omega x) + B^+ \sin(\omega x), \ x_j < x < 1 , \end{cases}$$

(6.6)

with suitable $A^\pm, B^\pm, A, B \in \mathbb{C}$. We used the abbreviations

$$s_j(x) := -(x - m_j)\frac{\sin(\omega(x - m_j))}{2\omega} \quad , \quad c_j(x) := (x - m_j)\frac{\cos(\omega(x - m_j))}{2\omega} ,$$

for $x_{j-1} < x < x_j$; these functions are supposed to be zero outside $]x_{j-1}, x_j[$.

Write Q_ω for the $L^2(]-1, 1[)$–orthogonal projection onto V_h, which is defined in a completely local fashion. Since it leaves local plane waves invariant, we find

$$\big((Id - \mathsf{Q}_\omega)\varphi_j\big)(x) = \begin{cases} (Id - \mathsf{Q}_\omega)(\rho_j s_j + \kappa_j c_j) & \text{for } x_{j-1} < x < x_j , \\ 0 & \text{elsewhere.} \end{cases}$$

(6.7)

As a consequence, the projection error allows a completely local analysis

$$(Id - \mathsf{Q}_\omega)\varphi = \sum_{j=1}^M (Id - \mathsf{Q}_\omega)(\rho_j s_j + \kappa_j c_j) .$$

(6.8)

Thanks to symmetries of the basis functions $\cos(\omega(x - m_j))$, $\sin(\omega(x - m_j))$, and s_j and c_j, one readily computes, with $\widehat{\omega} := \frac{1}{2} h_j \omega$, $h_j := x_j - x_{j-1}$, and for $x_{j-1} \le x \le x_j$,

$$\mathsf{Q}_\omega s_j(x) = -(\tfrac{1}{2} h_j)^2 \frac{\frac{1}{4} \widehat{\omega}^{-1} \int_{-1}^1 \xi \sin(2 \widehat{\omega} \xi) \, \mathrm{d}\xi}{\int_{-1}^1 \cos^2(\widehat{\omega} \xi) \, \mathrm{d}\xi} \cdot \cos(\omega(x - m_j)) \, , \qquad (6.9)$$

$$\mathsf{Q}_\omega c_j(x) = (\tfrac{1}{2} h_j)^2 \frac{\frac{1}{4} \widehat{\omega}^{-1} \int_{-1}^1 \xi \sin(2 \widehat{\omega} \xi) \, \mathrm{d}\xi}{\int_{-1}^1 \sin^2(\widehat{\omega} \xi) \, \mathrm{d}\xi} \cdot \sin(\omega(x - m_j)) \, . \qquad (6.10)$$

Eventually, we have to measure the projection error in the norm $\| \cdot \|_{DG+}$. The local contribution from the j–th cell $]x_{j-1}, x_j[$ is bounded by

$$\|(Id - \mathsf{Q}_\omega)\varphi\|_{DG+,j}^2 \le C \Big(\omega^2 \|(Id - \mathsf{Q}_\omega)\varphi_j\|_{0,]x_{j-1},x_j[}^2 + |(Id - \mathsf{Q}_\omega)\varphi_j|_{1,]x_{j-1},x_j[}^2 +$$
$$h_j^{-1} \left((Id - \mathsf{Q}_\omega)\varphi_j(x_{j-1})^2 + (Id - \mathsf{Q}_\omega)\varphi_j(x_j)^2 \right) +$$
$$h_j \left(((Id - \mathsf{Q}_\omega)\varphi_j)'(x_{j-1})^2 + ((Id - \mathsf{Q}_\omega)\varphi_j)'(x_j)^2 \right) \Big) \, .$$
$$(6.11)$$

For symmetry reasons, we have orthogonality with respect to the inner product associated with the local norm (6.11) between the basis functions $\cos(\omega(x - m_j))$ and $\sin(\omega(x - m_j))$, s_j and c_j, s_j and $\sin(\omega(x - m_j))$, c_j and $\cos(\omega(x - m_j))$. Hence, in order to determine the best possible constant in the estimate $\|(Id - \mathsf{Q}_\omega)\varphi\|_{DG+} \le C \|w_h\|_{0,]-1,1[}$, we have to compute

$$C^2 := \max_{1 \le j \le M} \max \left\{ \frac{\|(Id - \mathsf{Q}_\omega)s_j\|_{DG+,j}^2}{\| \cos(\omega \cdot) \|_{0,]x_{j-1},x_j[}^2}, \frac{\|(Id - \mathsf{Q}_\omega)c_j\|_{DG+,j}^2}{\| \sin(\omega \cdot) \|_{0,]x_{j-1},x_j[}^2} \right\} \, . \qquad (6.12)$$

Based on (6.9) and (6.10) we obtain

$$\omega^2 \|(Id - \mathsf{Q}_\omega)s_j\|_{0,]x_{j-1},x_j[}^2 = \tfrac{1}{4} (\tfrac{1}{2} h_j)^3 \left(\int_{-1}^1 \xi^2 \sin(\widehat{\omega} \xi)^2 \, \mathrm{d}\xi - \frac{\left(\int_{-1}^1 \xi \sin(2 \widehat{\omega} \xi) \, \mathrm{d}\xi \right)^2}{4 \int_{-1}^1 \cos^2(\widehat{\omega} \xi) \, \mathrm{d}\xi} \right) \, ,$$
$$(6.13)$$

$$\omega^2 \|(Id - \mathsf{Q}_\omega)c_j\|_{0,]x_{j-1},x_j[}^2 = \tfrac{1}{4} (\tfrac{1}{2} h_j)^3 \left(\int_{-1}^1 \xi^2 \cos(\widehat{\omega} \xi)^2 \, \mathrm{d}\xi - \frac{\left(\int_{-1}^1 \xi \sin(2 \widehat{\omega} \xi) \, \mathrm{d}\xi \right)^2}{4 \int_{-1}^1 \sin^2(\widehat{\omega} \xi) \, \mathrm{d}\xi} \right) \, .$$
$$(6.14)$$

This implies, for instance,

$$\frac{\omega^2 \|(Id - \mathsf{Q}_\omega)s_j\|_{0,]x_{j-1},x_j[}^2}{\| \cos(\omega \cdot) \|_{0,]x_{j-1},x_j[}^2} = (\tfrac{1}{2} h_j)^2 \left(\frac{\int_{-1}^1 \xi^2 \sin(\widehat{\omega} \xi)^2 \, \mathrm{d}\xi}{4 \int_{-1}^1 \cos^2(\widehat{\omega} \xi) \, \mathrm{d}\xi} - \left(\frac{\int_{-1}^1 \xi \sin(2 \widehat{\omega} \xi) \, \mathrm{d}\xi}{2 \int_{-1}^1 \cos^2(\widehat{\omega} \xi) \, \mathrm{d}\xi} \right)^2 \right) \, ,$$
$$(6.15)$$

$$\frac{\omega^2 \|(Id - \mathsf{Q}_\omega)c_j\|_{0,]x_{j-1},x_j[}^2}{\| \sin(\omega \cdot) \|_{0,]x_{j-1},x_j[}^2} = (\tfrac{1}{2} h_j)^2 \left(\frac{\int_{-1}^1 \xi^2 \cos(\widehat{\omega} \xi)^2 \, \mathrm{d}\xi}{4 \int_{-1}^1 \sin^2(\widehat{\omega} \xi) \, \mathrm{d}\xi} - \left(\frac{\int_{-1}^1 \xi \sin(2 \widehat{\omega} \xi) \, \mathrm{d}\xi}{2 \int_{-1}^1 \sin^2(\widehat{\omega} \xi) \, \mathrm{d}\xi} \right)^2 \right) \, .$$
$$(6.16)$$

Similar symbolic expressions can be derived for all other components of the norm $\|\cdot\|_{DG+,j}$. Thus we end up with an estimate of the form

$$\|(Id - \mathsf{Q}_\omega)\varphi_j\|^2_{DG+,j} \leq h_j^2 \eta(h_j\omega)\|w_h\|^2_{0,]x_{j-1},x_j[} \, , \tag{6.17}$$

for which the function η is available as a sum of expressions involving integrals over $[-1, 1]$ that can be computed in closed form. Here, we are content with its numerical evaluation. The behavior of η is displayed in Fig. 6.1. The most important observation is that η is *uniformly bounded* for all real arguments.
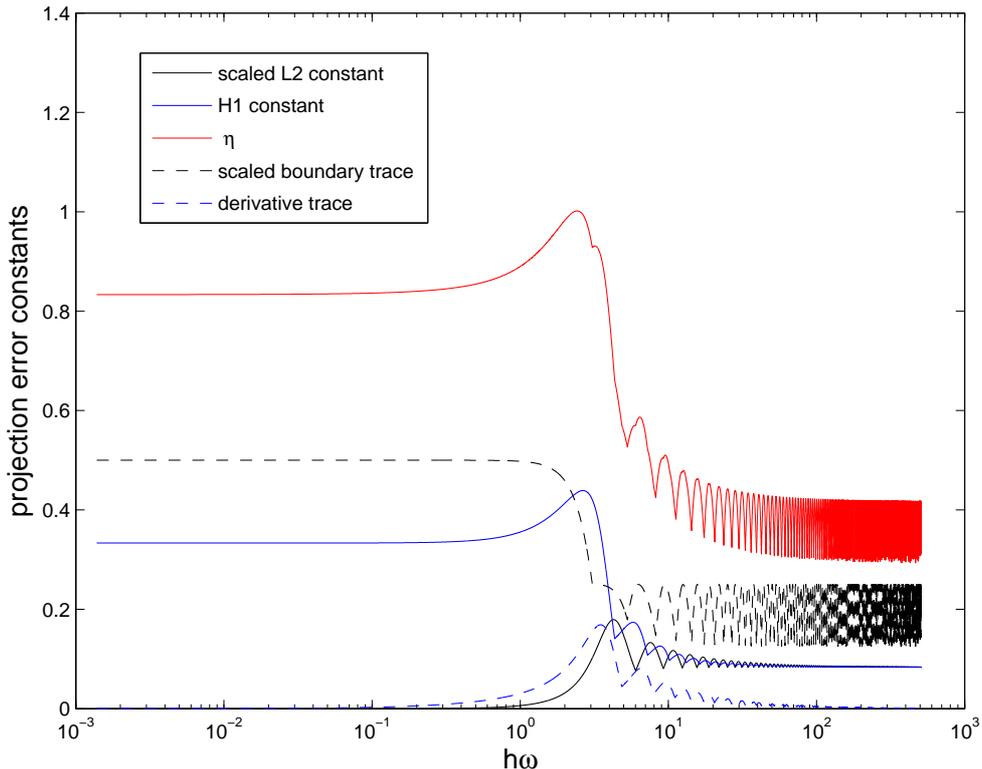
FIG. 6.1. *Function η from* (6.17)

Writing $h := \max_j h_j$ for the global mesh width, we conclude the duality estimate, *cf.* (5.21),

$$\omega|(u - u_h, w_h)| \leq Ch\omega\|w_h\|_{0,]-1,1[} \left(\|u - u_h\|_{DG} + \|f - \mathsf{Q}_\omega f\|_{0,]-1,1[}\right) \, . \tag{6.18}$$

with $C > 0$ independent of both the mesh and ω.

The important message sent by (6.18) and (5.8) is that quasi-optimality of Galerkin solutions can already be achieved by guaranteeing $Ch\omega < 1$, which constitutes a major improvement compared to the requirement $c_0 h\omega^2 < 1$ stipulated by the general analysis of Section 5. We owe this improvement to the exceptional possibility to capture all possible plane wave directions in one dimension. Thus the pollution effect can be avoided, as can also be achieved by other methods, see [4].

7. Numerical experiments. In a series of numerical experiments in 2D we study the convergence of the h-version of different primal plane wave discontinuous Galerkin methods. We consider (1.1) on simple bounded domains $\Omega \subset \mathbb{R}^2$ and fix source terms f and g such that u agrees with a prescribed analytic solution. All the computations were done in MATLAB on fairly uniform unstructured triangular meshes.

Experiment 1 studies the *homogeneous* Helmholtz boundary value problem (1.1) ($f = 0$) on the unit square $\Omega :=]0,1[^2$. We impose an outgoing cylindrical wave solution

$$u(\boldsymbol{x}) = H_0^{(1)}(\omega|\boldsymbol{x} - \boldsymbol{x}_0|) \,, \quad \boldsymbol{x}_0 = \begin{pmatrix} -1/4 \\ 0 \end{pmatrix} \,, \tag{7.1}$$

where $H_0^{(1)}$ is the zero-th order Hankel function of the first kind.

The experiment seeks to explore

1. the relative performance of different versions of the mixed discontinuous Galerkin approach (3.7), which differ in the choice of the parameters α, β, and γ in the numerical fluxes (3.10), (3.11), see Table 7.1. Note that UWVF does not, and PWDG0 may not comply with the assumptions of Propostion 5.2.
2. the presence and strength of the pollution effect, by monitoring the onset of asymptotic convergence and its dependence on ωh as well as the increase of the discretization error for increasing ω and fixed ωh.

A sequence of unstructured triangular meshes of different resolution (measured in terms of the maximal edge length h) was used. It was produced by a mesh generator. Figure 7.1 gives an impression of what these meshes look like. We measure the discretization error in the broken version of the weighted norm ("energy norm") (5.11)

$$\|v\|_{1,\omega,h}^2 := \|\nabla_h v\|_{0,\Omega}^2 + \omega^2 \|v\|_{0,\Omega}^2 \,, \tag{7.2}$$

and in the $L^2(\Omega)$-norm.
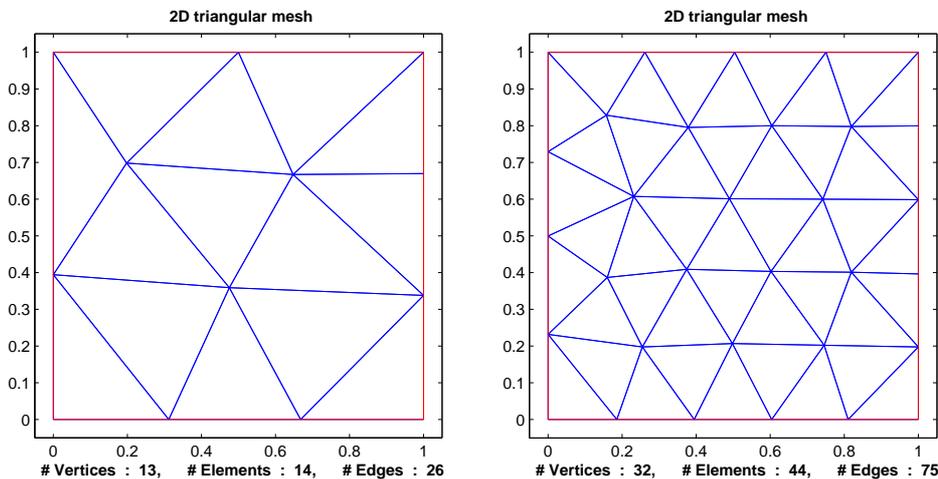
FIG. 7.1. *The third and fifth coarsest meshes on the unit square.*

We observe algebraic convergence in terms of $h\omega$ for all methods and $p = 5$, see Figures 7.2, 7.3. All the methods offer about the same accuracy and convergence rates.

method	α	β	γ	δ	λ
UWVF [9]	$\frac{1}{2}$	$\frac{1}{2}$	0	$\frac{1}{2}$	$\frac{1}{2}$
PWDG0	$\frac{2}{\omega h}$	0	0	0	$\frac{2}{\omega h}$
PWDG1	$\frac{C^2}{2\omega h}$	0	0	0	$\frac{C^2}{\omega h}$
PWDG2	$\frac{C^2}{2\omega h}$	$\frac{\omega h}{10}$	0	$\min\{\frac{1}{2}, \frac{\omega h}{10}\}$	$\frac{C^2}{\omega h}$

TABLE 7.1

Choice of parameters for numerical fluxes (3.10), (3.11), (3.13), with different plane wave DG methods. Here, C denotes an estimate for C_{tinv} from Thm. 4.7. We computed C_{tinv} on each element using (4.46) in the plane wave basis and defined C on each edge as the maximal value of C_{tinv} on the neighboring elements.

The plots hint at a slightly worse convergence for the classical UWVF, which does not comply with the assumptions of the theory of Sect. 5.
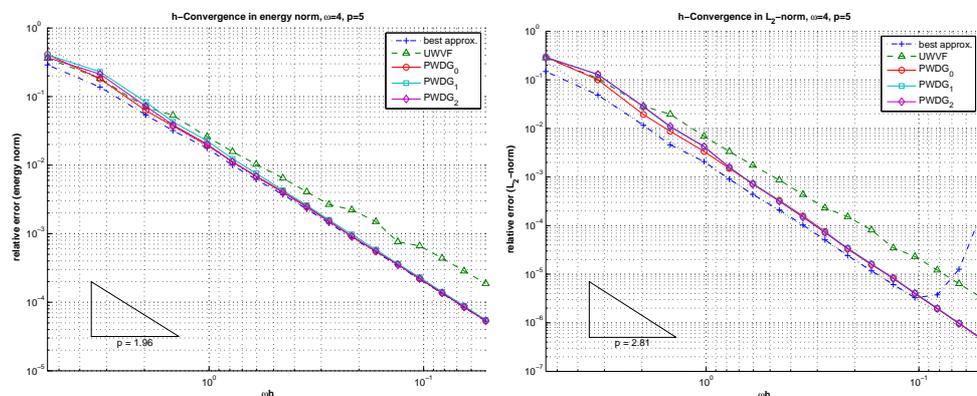
FIG. 7.2. *Experiment 1: h-convergence of PWDG methods for $\omega = 4$. The relative errors in the energy norm (7.2) and the L^2-norm are plotted against ωh. The divergence of the best approximation in the L^2-norm is due to numerical instability in the computation of the L^2-projection.*

In Figure 7.4 we notice faster algebraic convergence when using more plane wave directions in the local trial spaces, *cf.* Remark 5.12.

Figures 7.3 and 7.5 highlight delayed onset of algebraic convergence for high wavenumbers. Moreover, the plane wave DG solutions fails to come close to the best approximation of the exact solution in the trial space. Thus, keeping ωh small, which guarantees uniformly accurate best approximation in plane wave space, fails to control the Galerkin discretization error for increasing ω, see Figure 7.6. All this is clear evidence that numerical dispersion (pollution effect) also affects plane wave DG methods, *cf.* Remark 5.11.

Experiment 2 conducts similar investigations as Experiment 1 for the realistic setting of plane wave scattering at a sound soft circular object. Spatial discretization is carried out in an annulus $\Omega := \{\boldsymbol{x} \in \mathbb{R}^2 : 1 < |\boldsymbol{x}| < 3\}$ and the exterior inhomogeneous impedance boundary conditions allow for the exact Mie solution to the problem,

$$u(r, \varphi) = -\frac{J_0(\omega)}{H_0^{(2)}(\omega)} H_0^{(2)}(\omega r) - 2 \sum_{n=1}^{\infty} i^n \frac{J_n(\omega)}{H_n^{(2)}(\omega)} H_n^{(2)}(\omega r) \cos(n\varphi) . \qquad (7.3)$$
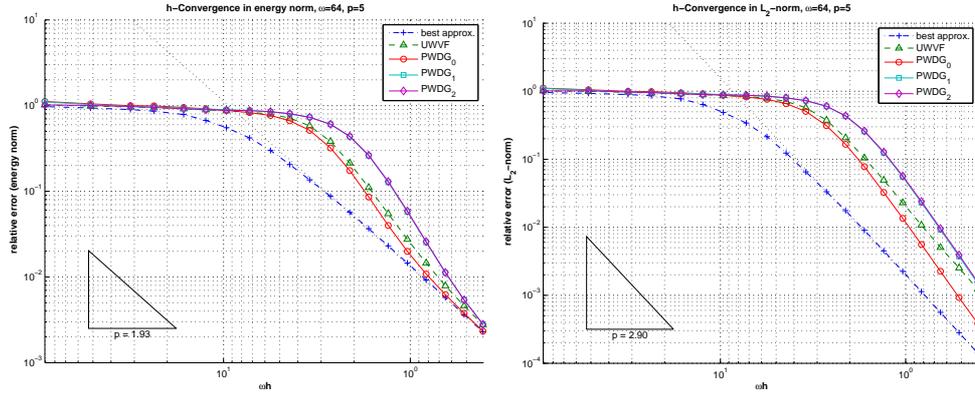
FIG. 7.3. *Experiment 1: h-convergence of PWDG methods for $\omega = 64$. The relative errors in the energy norm* (7.2) *and the L^2-norm are plotted against ωh.*
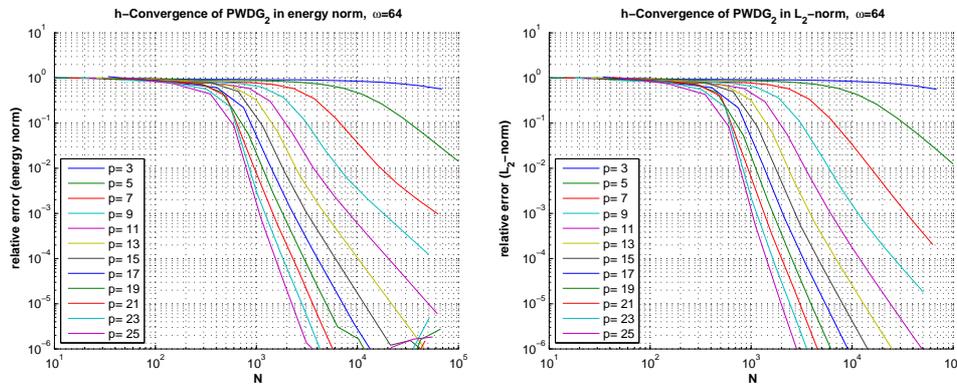

FIG. 7.4. *Experiment 1: h-convergence of PWDG2 for various values of p. The relative errors in the energy norm* (7.2) *and the L^2-norm are plotted against the number N of degrees of freedom.*
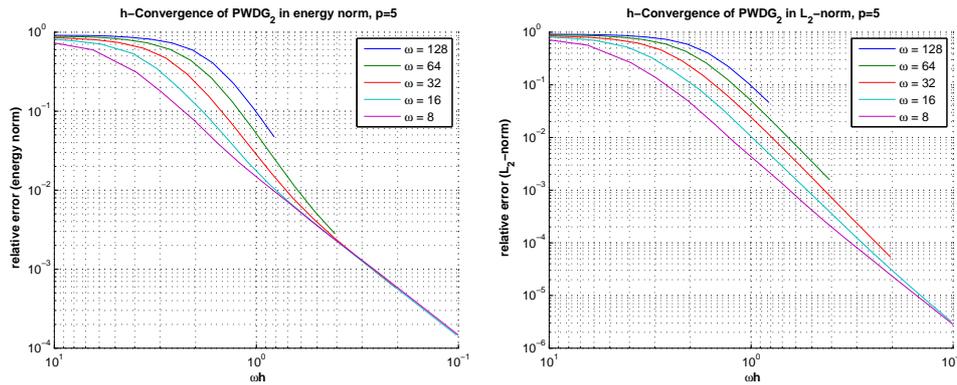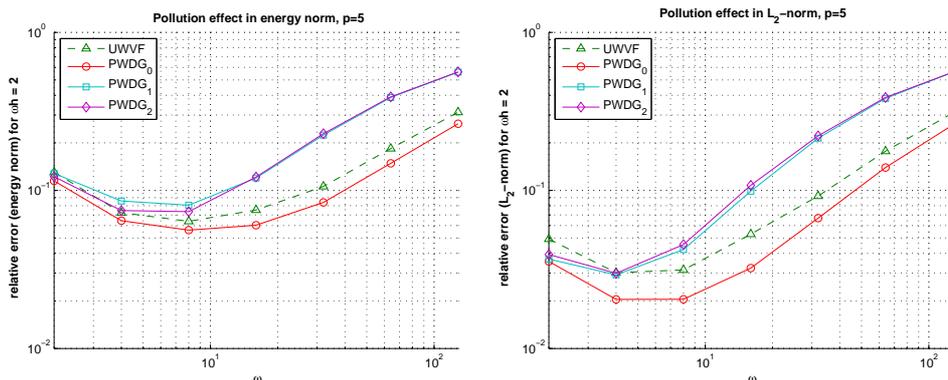

FIG. 7.5. *Experiment 1: h-convergence of PWDG2 for various values of ω. The relative errors in the energy norm* (7.2) *and the L^2-norm are plotted against ωh.*

FIG. 7.6. *Experiment 1: errors of PWDG methods for fixed* $\omega h = 2$ *and variable* ω. *Values were computed by linear interpolation (w.r.t. h) of data points in bilogarithmic scale.*

Dirichlet boundary conditions corresponding to the negative of the incoming wave $\exp(i\omega\binom{1}{0} \cdot \boldsymbol{x})$ are imposed on the inner circle.

The circular boundary is exactly taken into account by using an analytic parameterization. The evaluation of the matrix entries relies on high order Gaussian quadrature rules which produce negligible quadrature error for all wave numbers ω used in this experiment.
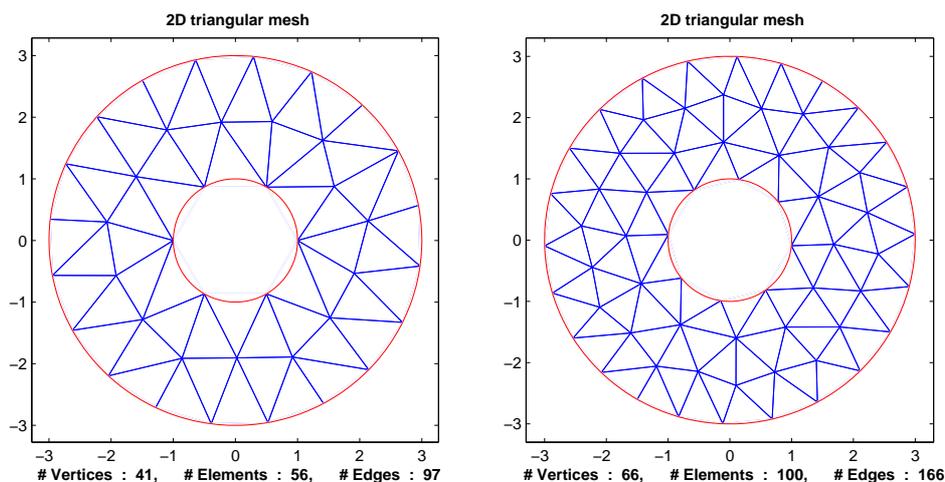
FIG. 7.7. *Experiment 2: the two coarsest meshes on the annulus.*

By and large, in Experiment 2 we make the same observations as in Experiment 1, see Figures 7.8 through 7.10.

Experiment 3 studies the *inhomogeneous* Helmholtz boundary value problem (1.1), i.e., $f \neq 0$. As solution we impose a circular wave (7.1) belonging to the "wrong" frequency $\frac{1}{2}\omega$. Again, $\Omega :=]0, 1[^2$.

Again, for $p = 5$, we observe algebraic convergence in ωh in all norms examined, see Figures 7.11 and 7.12. The classical UWVF suffers reduced order of convergence in $L^2(\omega)$-norm. Figure 7.13 demonstrates that for this inhomogeneous Helmholtz prob-
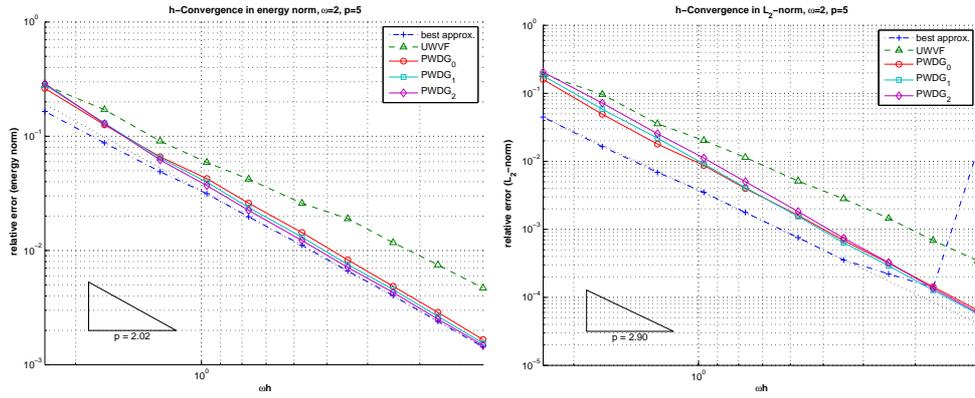
FIG. 7.8. *Experiment 2: h-convergence of PWDG methods for $\omega = 2$. The relative errors in the energy norm* (7.2) *and the L^2-norm are plotted against ωh.*
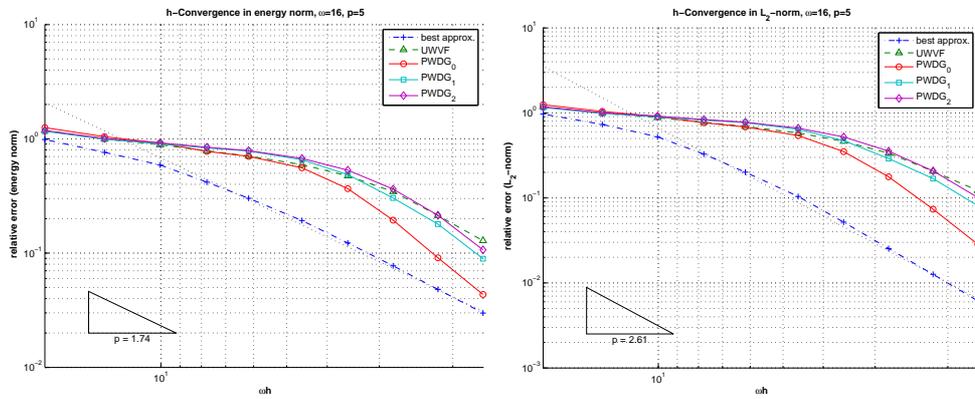

FIG. 7.9. *Experiment 2: h-convergence of PWDG2 for $\omega = 16$. The relative errors in the energy norm* (7.2) *and the L^2-norm are plotted against ωh.*
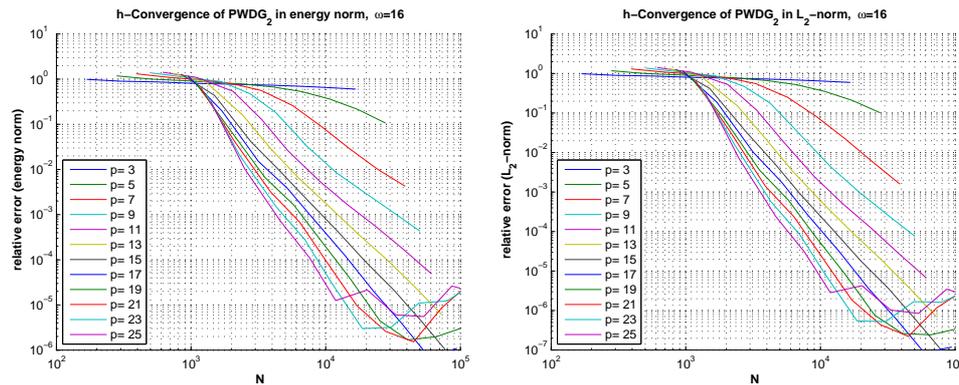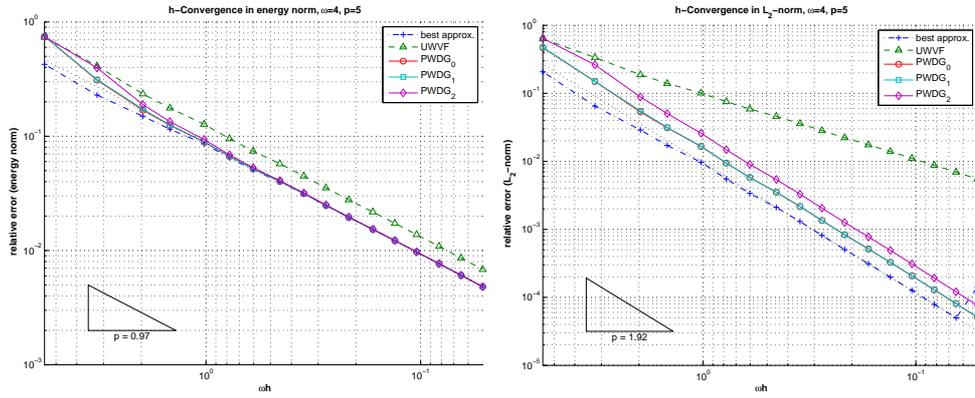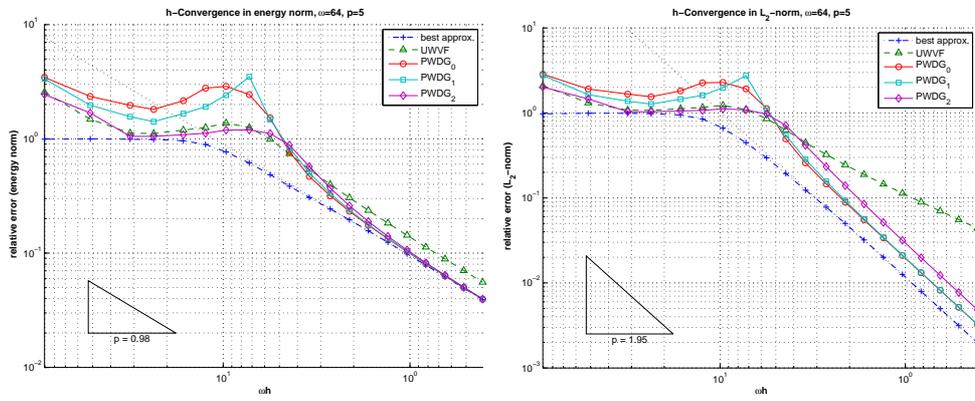

FIG. 7.10. *Experiment 2: h-convergence of PWDG2 for various values of p. The relative errors in the energy norm* (7.2) *and the L^2-norm are plotted against the number N of degrees of freedom.*

FIG. 7.11. *Experiment 3: h-convergence of PWDG methods for $\omega = 4$. The relative errors in the energy norm (7.2) and the L^2-norm are plotted against ωh.*

FIG. 7.12. *Experiment 3: h-convergence of PWDG methods for $\omega = 64$. The relative errors in the energy norm (7.2) and the L^2-norm are plotted against ωh.*
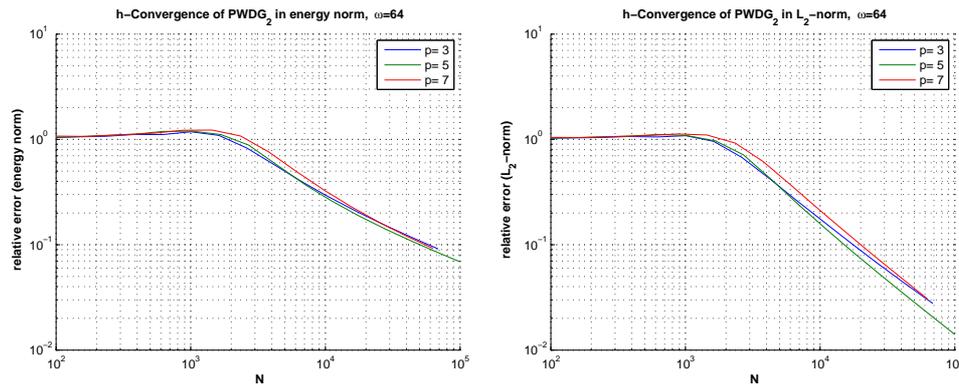

FIG. 7.13. *Experiment 3: h-convergence of PWDG2 for various values of p. The relative errors in the energy norm (7.2) and the L^2-norm are plotted against the number N of degrees of freedom.*
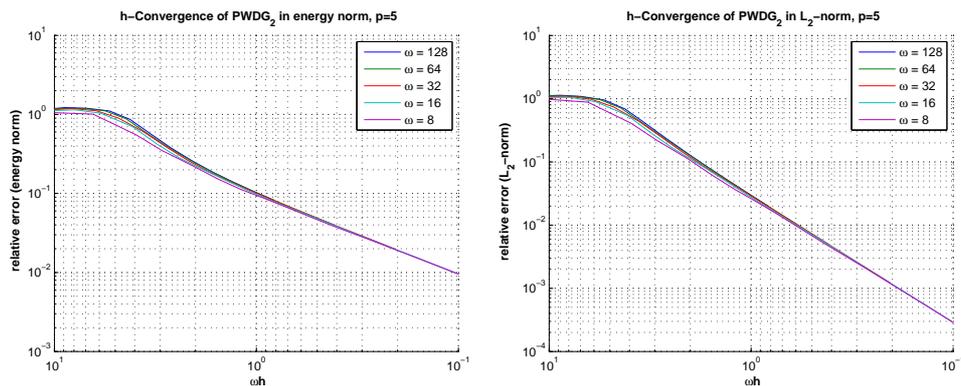
FIG. 7.14. *Experiment 3: h-convergence of PWDG2 for various values of ω. The relative errors in the energy norm* (7.2) *and the L^2-norm are plotted against ωh.*

lem raising p does not give better accuracy, *cf.* Remark 5.12.

However, since in this experiment the solution is not a propagating wave, numerical dispersion cannot impair accuracy, see Figure 7.14.

REFERENCES

[1] M. Ainsworth, *Discrete dispersion relation for hp-version finite element approximation at high wave number*, SIAM J. Numer. Anal., 42 (2004), pp. 563–575.

[2] D. Arnold, F. Brezzi, B. Cockburn, and L. Marini, *Unified analysis of discontinuous Galerkin methods for elliptic problems*, SIAM J. Numer. Anal., 39 (2002), pp. 1749–1779.

[3] I. Babuška and J. Melenk, *The partition of unity method*, Int. J. Numer. Methods Eng., 40 (1997), pp. 727–758.

[4] I. Babuška and S. Sauter, *Is the pollution effect of the FEM avoidable for the Helmholtz equation?*, SIAM Review, 42 (2000), pp. 451–484.

[5] L. Banjai and S. Sauter, *A refined Galerkin error and stability analysis for highly indefinite variational problems*, Report 03-06, Institut für Mathematik, Universität Zürich, Zürich, Switzerland, 2006.

[6] S. Brenner and R. Scott, *Mathematical theory of finite element methods*, Texts in Applied Mathematics, Springer–Verlag, New York, 2nd ed., 2002.

[7] A. Buffa and P. Monk, *Error estimates for the ultra weak variattional formulation of the helmholtz equation*, Math. Mod. Numer. Anal., (2007). Submitted.

[8] P. Castillo, B. Cockburn, I. Perugia, and D. Schötzau, *An a priori error analysis of the local discontinuous galerkin method for elliptic problems*, SIAM J. Numer. Anal., 38 (2000), pp. 1676–1706.

[9] O. Cessenat and B. Despres, *Application of an ultra weak variational formulation of elliptic PDEs to the two-dimensional Helmholtz equation*, SIAM J. Numer. Anal., 35 (1998), pp. 255–299.

[10] ———, *Using plane waves as base functions for solving time harmonic equations with the ultra weak variational formulation*, J. Computational Acoustics, 11 (2003), pp. 227–238.

[11] B. Despres, *Sur une formulation variationelle de type ultra-faible*, C.R. Acad. Sci. Paris, Ser. I, 318 (1994), pp. 939–944.

[12] C. Farhat, I. Harari, and U. Hetmaniuk, *A discontinuous galerkin method with lagrange multipliers for the solution of helmholtz problems in the mid-frequency regime*, Computer Methods in Applied Mechanics and Engineering, 192 (2003), pp. 1389–1419.

[13] C. Farhat, R. Tezaur, and P. Weidemann-Goiran, *Higher-order extensions of a discontinuous Galerkin method for mid-frequency Helmholtz problems*, Int. J. Numer. Meth. Engr., 61 (2004).

[14] R. Hiptmair and P. Ledger, *A quadrilateral edge element scheme with minimum dispersion*, Report 2003-17, SAM, ETH Zürich, Zürich, Switzerland, December 2003.

[15] T. Huttunen, M. Malinen, and P. Monk, *Solving maxwell's equations using the ultra weak*

variational formulation, J. Comp. Phys., (2006).

[16] T. Huttunen and P. Monk, *The use of plane waves to approximate wave propagation in anisotropic media*, J. Computational Mathematics, 25 (2007), pp. 350–367.

[17] T. Huttunen, P. Monk, and J. Kaipio, *Computational aspects of the ultra-weak variational formulation*, J. Comp. Phys., 182 (2002), pp. 27–46.

[18] F. Ihlenburg, *Finite Element Analysis of Acoustic Scattering*, vol. 132 of Applied Mathematical Sciences, Springer-Verlag, New York, 1998.

[19] O. Laghrouche, P. Bettes, and R. Astley, *Modelling of short wave diffraction problems using approximating systems of plane waves*, Int. J. Numer. Meth. Engr., 54 (2002).

[20] J. Melenk, *On Generalized Finite Element Methods*, PhD thesis, University of Maryland, USA, 1995.

[21] P. Monk and D. Wang, *A least squares method for the helmholtz equation*, Computer Methods in Applied Mechanics and Engineering, 175 (1999), pp. 121–136.

[22] E. Perrey-Debain, O. Laghrouche, and P. Bettess, *Plane-wave basis finite elements and boundary elements for three-dimensional wave scattering*, Phil. Trans. R. Soc. London A, 362 (2004), pp. 561–577.

[23] A. Schatz, *An observation concerning Ritz-Galerkin methods with indefinite bilinear forms*, Math. Comp., 28 (1974), pp. 959–962.

[24] C. Schwab, *p- and hp-Finite Element Methods. Theory and Applications in Solid and Fluid Mechanics*, Numerical Mathematics and Scientific Computation, Clarendon Press, Oxford, 1998.

[25] M. Stojek, *Least-squares Trefftz-type elements for the Helmholtz equation*, Int. J. Numer. Meth. Engr., 41 (1998), pp. 831–849.

[26] R. Tezaur and C. Farhat, *Three-dimensional discontinuous Galerkin elements with plane waves and lagrange multipliers for the solution of mid-frequency helmholtz problems*, Int. J. Numer. Meth. Engr., 66 (2006), pp. 796–815.